

AD A090676

AFWAL-TR-80-3009

EFFECTS OF BIRD ORIENTATION AT IMPACT ON LOAD PROFILE AND  
DAMAGE LEVEL

ANTONIOS CHALLITA  
BLAINE S. WEST

University of Dayton Research Institute  
Dayton, Ohio 45469

JUNE 1980



TECHNICAL REPORT AFWAL-TR-80-3009  
Final Report for Period February 1979 - July 1979

Approved for public release; distribution unlimited.

FLIGHT DYNAMICS LABORATORY  
AIR FORCE WRIGHT AERONAUTICAL LABORATORIES  
AIR FORCE SYSTEMS COMMAND  
WRIGHT-PATTERSON AIR FORCE BASE, OHIO 45433

DDC FILE COPY

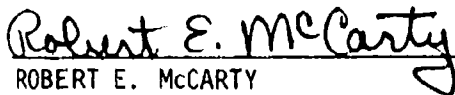
80 10 21 117


# NOTICE

When Government drawings, specifications, or other data are used for any purpose other than in connection with a definitely related Government procurement operation, the United States Government thereby incurs no responsibility nor any obligation whatsoever; and the fact that the government may have formulated, furnished, or in any way supplied the said drawings, specifications, or other data, is not to be regarded by implication or otherwise as in any manner licensing the holder or any other person or corporation, or conveying any rights or permission to manufacture, use, or sell any patented invention that may in any way be related thereto.

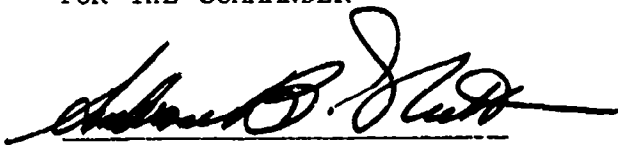
This report has been reviewed by the Information Office (OI) and is releasable to the National Technical Information Service (NTIS). At NTIS, it will be available to the general public, including foreign nations.

This technical report has been reviewed and is approved for publication.

  
ROBERT E. McCARTY  
Project Engineer

  
CHARLES V. MAYRAND, Acting Chief  
Crew Escape & Subsystems Branch  
Vehicle Equipment Division

FOR THE COMMANDER

  
AMBROSE B. NUTT  
Director  
Vehicle Equipment Division

Copies of this report should not be returned unless return is required by security considerations, contractual obligations, or notice on a specific document.

UNCLASSIFIED

SECURITY CLASSIFICATION OF THIS PAGE (When Data Entered)

REPORT DOCUMENTATION PAGE		READ INSTRUCTIONS BEFORE COMPLETING FORM
1. REPORT NUMBER	2. GOVT ACCESSION NO.	3. RECIPIENT'S CATALOG NUMBER
AFWAL-TR-80-3009 ✓	AD-A090676	
4. TITLE (and Subtitle)		5. TYPE OF REPORT & PERIOD COVERED
Effects of Bird Orientation at Impact on Load Profile and Damage Level		Final Technical Report. Feb 1979 - July 1979
7. AUTHOR(s)		6. PERFORMING ORG. REPORT NUMBER
Antonios, Challita Blaine S./West		UDR-TR-79-63 ✓
9. PERFORMING ORGANIZATION NAME AND ADDRESS		6. CONTRACT OR GRANT NUMBER(s)
University of Dayton Research Institute 300 College Park Avenue Dayton, Ohio 45469 ✓		F33615-78-C-3402 ✓
11. CONTROLLING OFFICE NAME AND ADDRESS		10. PROGRAM ELEMENT, PROJECT, TASK AREA & WORK UNIT NUMBERS
Air Force Flight Dynamics Laboratory AF Wright Aeronautical Labs, AFSC Wright-Patterson Air Force Base, OH 45433		Prog. Ele. 62201F Proj. 2402, Task 240203 Work Unit 24020318
14. MONITORING AGENCY NAME & ADDRESS (if different from Controlling Office)		12. REPORT DATE
		June 1980
		13. NUMBER OF PAGES
		86
		15. SECURITY CLASS. (of this report)
		Unclassified
		15a. DECLASSIFICATION DOWNGRADING SCHEDULE
16. DISTRIBUTION STATEMENT (of this Report)		
Approved for public release; distribution unlimited.		
17. DISTRIBUTION STATEMENT (of the abstract entered in Block 20, if different from Report)		
18. SUPPLEMENTARY NOTES		
19. KEY WORDS (Continue on reverse side if necessary and identify by block number)		
foreign object damage, bird impact, transverse orientations, transparencies, worst-case orientation, minimum perforation velocity, bird loading, polycarbonate panels		
20. ABSTRACT (Continue on reverse side if necessary and identify by block number)		
This report describes an experimental study which was conducted to investigate the effects of bird orientation at impact and to identify the worst-case impact. 450 g substitute birds were launched with three different orientations onto 0.635 cm thick polycarbonate panels at four different locations. The minimum perforation velocity was used as the main criterion to measure damage; however, perforation wasn't achieved at the center of the		

DD FORM 1 JAN 73 1473

UNCLASSIFIED

SECURITY CLASSIFICATION OF THIS PAGE (When Data Entered)

UNCLASSIFIED

SECURITY CLASSIFICATION OF THIS PAGE(When Data Entered)

20.

panel and at the lower, or up-stream, corner. Therefore, another measure of damage was adopted for these locations; length of cracks, depth of pocket, etc. The end-on, or axial, orientation was found to be the most damaging orientation. Substitute birds were also launched with the two transverse orientations onto a rigid target plate at three obliquity angles, 90°, 45°, and 25°. Impact pressures were measured, and analyzed. Pressure profiles showed shock pressure only. No steady-state pressures were observed. Shock pressures were compared to theoretical Hugoniot curves and good agreements were obtained.

UNCLASSIFIED

SECURITY CLASSIFICATION OF THIS PAGE(When Data Entered)

## FOREWORD

The work effort described herein was conducted for the Flight Dynamics Laboratory under Contract F33615-78-C-3402. The project monitor was Mr. Robert E. McCarty. The experimental portion of the effort was conducted by the Impact Physics Group at the University of Dayton Research Institute. Mr. Blaine West and Dr. John Barber contributed to planning the experiments and analyzed the data. Mr. Antonios Challita supervised the experiments, while Mr. George Ahrens was the lead technician responsible for the conduct of the tests. Mr. George Roth served as the Project Supervisor for the University.

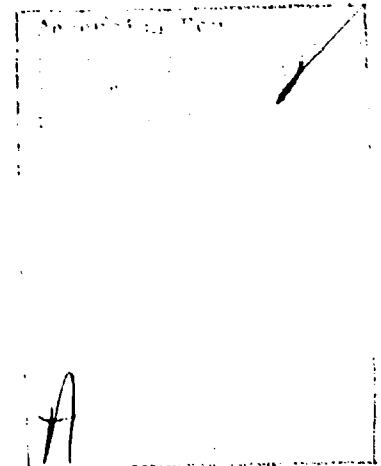


## TABLE OF CONTENTS

SECTION		PAGE
I	INTRODUCTION	1
	1. Background Information	1
	2. Program Objectives	3
II	EXPERIMENTAL TECHNIQUES	5
	1. Launch Techniques	5
	a. Transverse Orientation Launch System	5
	b. Axial Orientation Launch System	8
	2. Target Description	10
	3. Velocity, Location, and Orientation Measurement	12
	4. Pressure Measurements and Recording	14
III	EXPERIMENTAL RESULTS	17
	1. Bird Loading Studies	17
	a. Pressure-Time History	19
	b. Impact Phases	20
	(1) Initial Impact Pressure	23
	(2) Impact Pressure Decay	24
	c. Impact Duration	27
	2. Damage Potential Studies	30
	a. Factors Affecting Damage	32
	b. Summary of Results	33
IV	CONCLUSIONS AND RECOMMENDATIONS	42
	APPENDIX	43
	REFERENCES	71

# LIST OF ILLUSTRATIONS

FIGURE		PAGE
1	Foam Plastic Sabot used for Launching Transverse Birds	7
2	Overall View of the 177.8 mm Gun Range	8
3	Overall View of the 88.9 mm Gun Range	9
4	Foam Plastic Sabot used for Launching Axial Birds	10
5	Pressure Plate Mounted for Normal Impacts	11
6	Support Structure and Mounting Frame used with the 88.9 mm Gun	13
7	Support Structure and Mounting Frame used with the 177.8 mm Gun	13
8	X-radiograph of a 450 g Transversely Oriented Bird Substitute in Free-Flight. (a) from x-ray head along major axis of bird; (b) from x-ray head normal to major axis of bird	15
9	Bird Orientations for Oblique Transverse Impacts. The Upper Projectile Illustrates a Side-On Impact; the Lower Projectile Illustrates a Flat-On Impact.	18
10	Typical Pressure-Time Record of Nominal 450 g Bird Substitute (gelatin with 10% porosity) from Impacts with Flat-On Orientation. (a) 90° impact, 1" left of center; (b) 45° impact, 2" below center; (c) 25° impact, center transducer	21
11	Typical Pressure-Time Record of Nominal 450 g Bird Substitute (gelatin with 10% porosity) from Impacts with Side-On Orientation. (a) 90° impact, center transducer; (b) 45° impact, 2" below center; (c) 25° impact, 3" below center	22
12	Comparison of Measured Peak Pressures of 450 g Gelatin, Transverse Impacts at 90°, to Theoretical Shock Pressure Curve	25

# LIST OF ILLUSTRATIONS (CONTINUED)

FIGURE		PAGE
13	Comparison of Measured Peak Pressures of 450 g Gelatin, Transverse Impacts at 45°, to Theoretical Shock Pressure Curve	25
14	Comparison of Measured Peak Pressures of 450 g Gelatin, Transverse Impacts at 25°, to Theoretical Shock Pressure Curve	26
15	(a) Oblique Impact Effective Bird Length, End-On; (b) Oblique Impact Effective Bird Length, Flat-On; (c) Oblique Impact Effective Bird Length, Side-On	28
16	Acceptable Rotation. $\alpha$ is the Maximum Allowable Rotation. $\alpha$ is Measured in the Plane of the Target Plate	29
17	Polycarbonate Panel Bolted to the Structure	30
18	Impact Locations of Bird Substitute onto Polycarbonate Panels	31
A-1	Shot No. 4-0063; Panel Impacted at the Center Edge; One-Pound Gelatin Launched with an Axial Orientation at 204 m/s. a) Front View; b) End View	44
A-2	Shot No. 4-0064; Panel Impacted at the Center Edge; One-Pound Gelatin Launched with an Axial Orientation at 212 m/s. a) Front View; b) End View	45
A-3	Shot No. 4-0065; Panel Impacted at the Center Panel; One-Pound Gelatin Launched with an Axial Orientation at 290 m/s. a) Front View; b) End View	46
A-4	Shot No. 4-0067; Panel Impacted at the Center Panel; One-Pound Gelatin Launched with an Axial Orientation at 307 m/s. a) Front View; b) End View	47



# LIST OF ILLUSTRATIONS (CONTINUED)

FIGURE		PAGE
A-5	Shot No. 4-0072; Panel Impacted at the Down-Stream Corner; One-Pound Gelatin Launched with an Axial Orientation at 171 m/s. a) Front View; b) End View	48
A-6	Shot No. 4-0073; Panel Impacted at the Down-Stream Corner; One-Pound Gelatin Launched with an Axial Orientation at 175 m/s. a) Front View; b) End View	49
A-7	Shot No. 4-0076; Panel Impacted at the Up-Stream Corner; One-Pound Gelatin Launched with an Axial Orientation at 313 m/s. a) Front View; b) End View	50
A-8	Shot No. 4-0077; Panel Impacted at the Up-Stream Corner; One-Pound Gelatin Launched with an Axial Orientation at 303 m/s. a) Front View; b) End View	51
A-9	Shot No. 5-0147; Panel Impacted at the Center Edge; One-Pound Gelatin Launched with a Flat-On Orientation at 202 m/s. a) Front View; b) End View	52
A-10	Shot No. 5-0149; Panel Impacted at the Center Edge; One-Pound Gelatin Launched with a Flat-On Orientation at 206 m/s. a) Front View; b) End View	53
A-11	Shot No. 5-0150; Panel Impacted at the Center Panel; One-Pound Gelatin Launched with a Flat-On Orientation at 297 m/s. a) Front View; b) End View	54
A-12	Shot No. 5-0151; Panel Impacted at the Center Panel; One-Pound Gelatin Launched with a Flat-On Orientation at 307 m/s. a) Front View; b) End View	55
A-13	Shot No. 5-0152; Panel Impacted at the Center Panel; One-Pound Gelatin Launched with a Flat-On Orientation at 336 m/s. a) Front View; b) End View	56

# LIST OF ILLUSTRATIONS (CONTINUED)

FIGURE		PAGE
A-14	Shot No. 5-0155; Panel Impacted at the Center Panel; One-Pound Gelatin Launched with a Side-On Orientation at 292 m/s. a) Front View; b) End View	57
A-15	Shot No. 5-0157; Panel Impacted at the Center Panel; One-Pound Gelatin Launched with a Side-On Orientation at 333 m/s. a) Front View; b) End View	58
A-16	Shot No. 5-0158; Panel Impacted at the Center Edge; One-Pound Gelatin Launched with a Side-On Orientation at 210 m/s. a) Front View; b) End View	59
A-17	Shot No. 5-0160; Panel Impacted at the Center Edge; One-Pound Gelatin Launched with a Side-On Orientation at 212 m/s. a) Front View; b) End View	60
A-18	Shot No. 5-0162; Panel Impacted at the Center Edge; One-Pound Gelatin Launched with a Side-On Orientation at 210 m/s. a) Front View; b) End View	61
A-19	Shot No. 5-0164; Panel Impacted at the Center Edge; One-Pound Gelatin Launched with a Side-On Orientation at 212 m/s. a) Front View; b) End View	62
A-20	Shot No. 5-0166; Panel Impacted at the Down-Stream Corner; One-Pound Gelatin Launched with a Flat-On Orientation at 181 m/s. a) Front View; b) End View	63
A-21	Shot No. 5-0167; Panel Impacted at the Down-Stream Corner; One-Pound Gelatin Launched with a Flat-On Orientation at 188 m/s. a) Front View; b) End View	64
A-22	Shot No. 5-0175; Panel Impacted at the Down-Stream Corner; One-Pound Gelatin Launched with a Side-On Orientation at 237 m/s. a) Front View; b) End View	65
A-23	Shot No. 5-0177; Panel Impacted at the Down-Stream Corner; One-Pound Gelatin Launched with a Side-On Orientation at 232 m/s. a) Front View; b) End View	66

# LIST OF ILLUSTRATIONS (CONCLUDED)

FIGURE		PAGE
A-24	Shot No. 5-0178; Panel Impacted at the Up-Stream Corner; One-Pound Gelatin Launched with a Flat-On Orientation at 350 m/s. a) Front View; b) End View	67
A-25	Shot No. 5-0179; Panel Impacted at the Up-Stream Corner; One-Pound Gelatin Launched with a Flat-On Orientation at 335 m/s. a) End View; b) End View	68
A-26	Shot No. 5-0181; Panel Impacted at the Up-Stream Corner; One-Pound Gelatin Launched with a Flat-On Orientation at 305 m/s. a) Front View; b) End View	69
A-27	Shot No. 5-0184; Panel Impacted at the Up-Stream Corner; One-Pound Gelatin Launched with a Side-On Orientation at 306 m/s. a) Front View; b) End View	70

## LIST OF TABLES

TABLE		PAGE
1	Test Summary	34

# LIST OF UNITS

Mass	g (gram)	= 0.0022 lb <sub>m</sub> (pound-mass)
	kg (kilogram)	= 10 <sup>3</sup> g
Length	m (meter)	= 3.2808 ft (feet)
		= 39.37 in (inches)
	cm (centimeter)	= 0.01 m
		= 0.3937 in
	mm (millimeter)	= 0.001 m
Time	s (second)	
	μs (microsecond)	= 10 <sup>-6</sup> s
Force	N (Newton)	= 0.2248 lb <sub>f</sub> (pounds-force)
	MN (Meganewton)	= 10 <sup>6</sup> N
Density	kg/m <sup>3</sup>	= 0.0624 lb <sub>m</sub> /ft <sup>3</sup>
		= 3.613 x 10 <sup>-5</sup> lb <sub>m</sub> /in <sup>3</sup>
Pressure	MN/m <sup>2</sup>	= 10 bars
		= 145.04 lb <sub>f</sub> /in <sup>2</sup>
Frequency	H <sub>z</sub> (hertz)	
	kH <sub>z</sub> (kilohertz)	= 10 <sup>3</sup> H <sub>z</sub>

# LIST OF SYMBOLS

$d$	Bird diameter
ID	Inside diameter
$l$	Bird length
$l_{eff}$	Effective bird length
$m$	Bird mass
OD	Outside diameter
$P, P_p$	Measured peak pressure
$P_H$	Hugoniot pressure
$t$	Time
$T_s$	Impact duration
$V$	Impact velocity
$V_n$	Normal component of impact velocity
$V_s$	Shock Velocity
$\rho$	Density of projectile
$\theta$	Angle of impact

## SECTION I

### INTRODUCTION

#### 1. BACKGROUND INFORMATION

Aircraft and birds operate in the same space. Therefore, collisions between birds and aircraft are inevitable. Efforts have been made to reduce the possibility of collision by controlling the movement of birds and by changing the flight paths of aircraft. These actions have, in some instances, reduced the probability of collisions. However, in recent years the problem has been magnified by the introduction of an increased amount of high speed-low altitude flight time. This usage not only greatly increases the probability of a strike (through the sweeping out of a large volume of space in a high bird density regime) but it also greatly increases the impact energy associated with a given strike (the kinetic energy is a function of the square of the relative velocity at impact).

As a result of an increasing number of catastrophic bird-aircraft collisions the United States Air Force has initiated a number of programs with the objective of developing and applying the technology required to protect aircraft against birdstrike. The two areas of technology directly affected by the studies reported herein are; (1) characterization of the loads generated during a birdstrike, and (2) the testing procedures used to evaluate the level of birdstrike protection afforded by a given flight hardware system.

A number of investigations have been conducted to interpret bird impact with nonsteady fluid-dynamics and to characterize the transient loads exerted on the impacted structure. These investigations included real and substitute birds ranging in size from 60 to 3600 g. Target obliquity angles were 90 degrees, 45 degrees, or 25 degrees, and impact velocities ranged from 50 m/s to 300 m/s.

The University's effort to measure and characterize the loads exerted by birds during impact was begun in January 1974. This work was jointly sponsored by the Air Force Materials Laboratory (AFML) and the Air Force Flight Dynamics Laboratory (AFFDL). The initial work included development of basic experimental techniques and was reported by Barber in Reference 1. His report concentrated on normal impact of small birds (120 g). The work was extended to oblique impacts during a follow-on effort, in which pressure data were obtained at obliquities of 45 degrees and 25 degrees. Those results were reported in detail by Peterson in Reference 5. Then, these results provided a basis for identification of the fundamental processes affecting bird impact, as reported by Barber in Reference 2 and by Wilbeck in Reference 4. The first satisfactory bird impact flow model, featuring techniques necessary for proper scaling of the impact loads with bird size, was reported in Reference 2. Challita, in Reference 3, showed that the scaling relationships derived by Barber adequately described the impact process for bird masses ranging from 60 to 3600 g.

All of the work reported above was conducted with birds having nominal end-on orientation at impact. However, during the initial phases of these studies the orientation of some of the

- 
1. Barber, J. P., and Wilbeck, J. S., "The Characterization of Bird Impacts on a Rigid Plate: Part I", AFFDL-TR-75-5, ADA021142, January 1975.
  2. Barber, J. P., Taylor, H. R., and Wilbeck, J. S., "Bird Impact Forces and Pressures on Rigid and Compliant Targets," AFFDL-TR-77-60, ADA061-313, May 1978.
  3. Challita, A., and Barber, J. P., "The Scaling of Bird Impact Loads," AFFDL-TR-79-3042, June 1979.
  4. Wilbeck, T. S., "Impact Behavior of Low Strength Projectiles." AFML-TR-77-134, July 1978.
  5. Peterson, R. L., and Barber, J. P., "Bird Impact Forces in Aircraft Windshield Design," AFFDL-TR-75-150, ADA026-628, March 1976.



birds at impact was not well controlled. Results of those tests seemed to demonstrate that orientation at impact can have very pronounced effects on the magnitude, duration, and spatial distribution of impact induced loads.

Structural response analyses and testing experience have demonstrated that the birdstrike resistance of flight hardware is greatly influenced by the location of the impact point relative to the support structure, by the structural response characteristics of the support structure, and by the structural integrity of the panel/support structure interface.

Birdstrike testing procedures employed during developmental and/or qualification testing of full scale flight hardware have specified end-on orientation of the bird at the time of impact. However, in view of the preliminary early test results, it is not clear that the axial, or end-on, impacts qualification testing represent the most severe test condition for all impact locations and all structural system configurations. It is clear, however, that birds will strike aircraft transparencies with a random orientation and axial impacts have a rather low probability of occurrence.

## 2. PROGRAM OBJECTIVES

The program described in this report consisted of two primary experimental tasks. The objective of the first task was to determine the sensitivity of impact parameters to bird orientation. The investigation included both the temporal and spatial aspects of the loads. This was accomplished by measuring the loads produced by bird substitutes impacting a rigid flat target at two controlled transverse orientations. Specifically, 450 g bird substitutes were impacted at three impact angles (90, 45, and 25 degrees) and at three velocities (100, 200, and 300 m/s).

The objective of the second task was to investigate the damage potential of birds impacting a flat polycarbonate panel as a function of bird orientation at impact and impact location.

To achieve this objective 450 g bird substitutes were impacted on a 90 x 60 x 0.635 cm polycarbonate panel at a 25 degree angle of incidence. Three bird orientations (one axial plus two transverse) and four impact locations (center, edge, and two corners) were investigated.

## SECTION II

### EXPERIMENTAL TECHNIQUES

The experimental work described in this report was conducted at the University of Dayton Research Institute. This section contains a description of the experimental techniques used to launch 450 g bird substitutes (gelatin with 10 percent porosity) with controlled orientation onto nominal 0.635 cm flat polycarbonate panels. The techniques used to obtain temporally resolved rigid plate pressure measurements during bird impact with transverse orientations is also described. Descriptions of the experimental ranges and launch techniques, target structure and instrumentation, and data collection are given in the sections that follow.

#### 1. LAUNCH TECHNIQUES

For experimental investigations of bird impact onto a rigid target plate and onto a polycarbonate panel, launch techniques are necessary which can accelerate the 450 g birds with the required orientation to the required velocities. Birds must be launched with controlled orientation (transverse or axial), and such that they do not break up or severely distort prior to impact. Launch techniques were developed such that birds with transverse orientation could be launched at velocities up to approximately 350 m/s, and birds with axial orientation at velocities up to approximately 300 m/s.

Two systems were used: a 177.8 mm bore compressed air gun to launch birds with transverse orientation and a 88.9 mm bore compressed air gun to launch birds with axial orientation. A description of both systems follows.

##### a. Transverse Orientation Launch System

This system consisted of a 177.8 mm bore compressed air gun with supporting compressor, instrumentation, and control

systems. The compressor system consisted of a  $1.42 \text{ m}^3/\text{min}$ ,  $3.5 \text{ MN/m}^2$  compressor pumping into a  $0.11 \text{ m}^3$  intermediate storage tank. The intermediate storage tank was connected via a flexible hose and quick disconnect coupler to the  $0.85 \text{ m}^3$  air storage tank used for driving the gun. A valve system is located between the driving air storage tank and the breech of the gun. This valve was designed to valve the high pressure air from the driving storage tank into the gun to operate it. The valve was a standard butterfly valve system with a pneumatic actuator.

The gun itself consisted of two 4.88 m long, 177.8 mm ID heavy wall tubes. They were connected via a locating ring and flange system. The tubes were supported on two heavy I-beams bolted to the floor. A vent section was connected to the muzzle of the gun tube and was designed to release the driving pressure from the back of the projectile package. This vent section was enclosed in a muffler which deflected the venting gases harmlessly toward the floor.

The birds were placed in a sabot, or carrier, for launching. The sabot was a 177.8 mm OD foam plastic cylinder with a transverse pocket in front in the shape of a right circular cylinder cut in half along its axis. This pocket was designed to accept the bird which was to be launched in the transverse orientation. The sabot is shown in Figure 1. Foam plastic was employed because it is lightweight, strong and very dimensionally stable.

As the sabot represents a significant fraction of the launch mass, it must be stripped from the bird before the bird impacts the target. Accordingly, a tapered tube sabot stripping section was connected to the muzzle end of the vent section. The sabot stripper tube consisted of a steel tube with an initial ID of 177.8 mm that was progressively reduced. A series of longitudinal wide slots were cut into the stripper tube to facilitate the rapid release of the driving pressure, thus

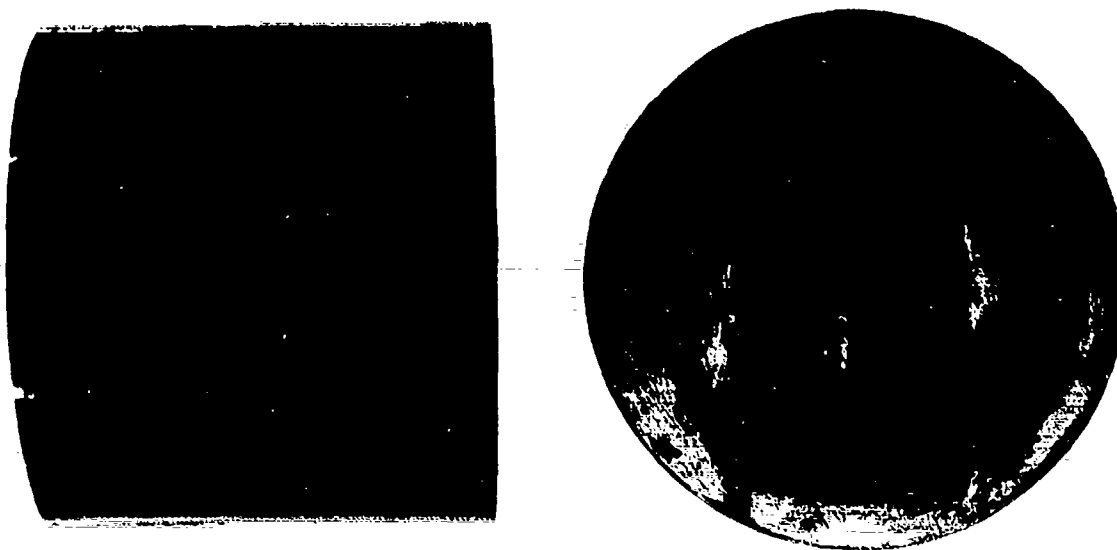


Figure 1. Foam Plastic Sabot Used for Launching Transverse Birds.

reducing the forces required to decelerate and stop the sabot. When the launch package entered the sabot stripper tube, the sabot was progressively decelerated until it stopped. The bird, released from the sabot pocket, continued on trajectory to the target. The sabot stripper section functioned satisfactorily over the range of velocities below 300 m/s. The sabot broke into pieces, when the velocities were higher than 300 m/s, without affecting the trajectory or the orientation of the bird.

Spinning of the projectile was detected in the early development shots. A thorough investigation was conducted and the source initiating the spinning was determined and eliminated during the test shots. It was found that the spinning was caused by a slight rifling action in the barrel, instability of the package (sabot and projectile), i.e., center of gravity of the package was off the center line of trajectory, and by the fact that the sabot and the barrel were not perfectly

circular or concentric. Different techniques were used to eliminate the spinning. Some of these techniques were: compensating for the spinning by loading the package at a predetermined angle, stabilizing the package by inserting a heavy weight in the bottom part of the sabot, and using a 3.175 mm diameter wire rope as a rail to guide the sabot. The last technique was the most efficient; it kept the rotation within acceptable limits. A justification of the acceptable limits is given in later sections. The wire rope proved completely satisfactory for controlling orientations over the entire range of velocities used in this study. An overall view of the 177.8 mm gun is shown in Figure 2.

b. Axial Orientation Launch System

The 88.9 mm bore compressed air gun consisted of a 3.66 m long tube supported on two heavy I-beams bolted to

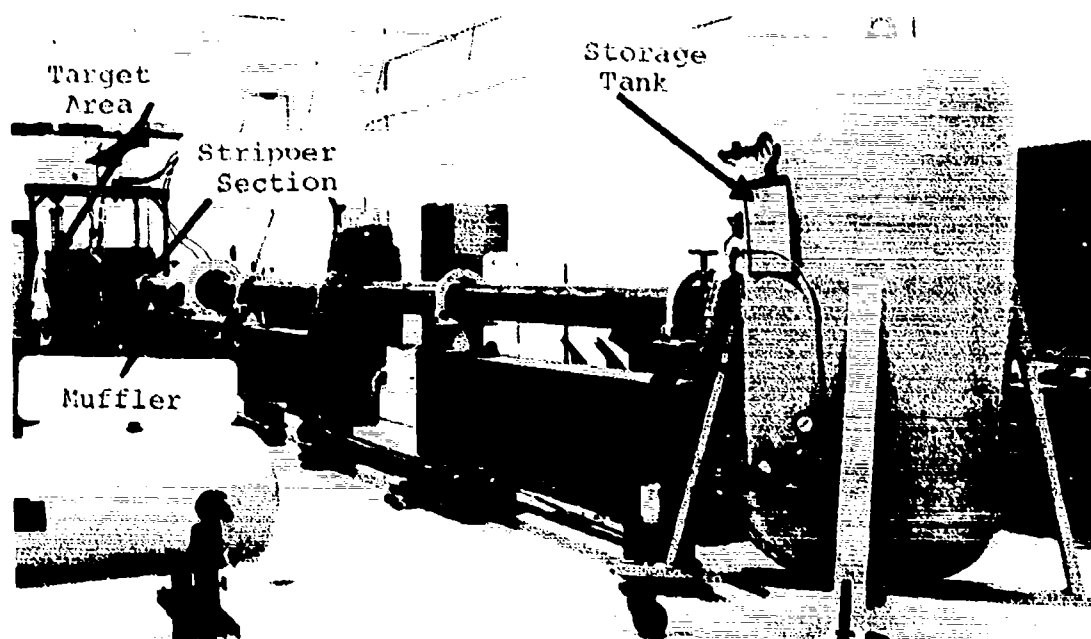


Figure 2. Overall View of the 177.8 mm Gun Range.

the floor. It uses the same compressor and intermediate storage tank as the 177.8 mm gun, and a similar air storage tank for driving the gun. The driving air storage tank had a capacity of approximately  $0.32 \text{ m}^3$ . A standard butterfly valve system with a pneumatic actuator was used to valve the high pressure air from the driving storage tank into the gun to operate it. A sabot stripper section was attached to the muzzle of the launcher. The sabot stripper tube consisted of a 88.9 mm ID steel tube with a series of longitudinal slits cut into it. Compression rings were placed around the outside of the tube and the ID of the tube was progressively reduced. For the high velocity shots an extension to the stripper tube was required. The tube was extended from its standard length of 3.05 m to a total length of 4.88 m. The sabot stripper functioned satisfactorily over the entire range of velocities which were used in this program. An overall view of the 88.9 mm launcher is shown in Figure 3.

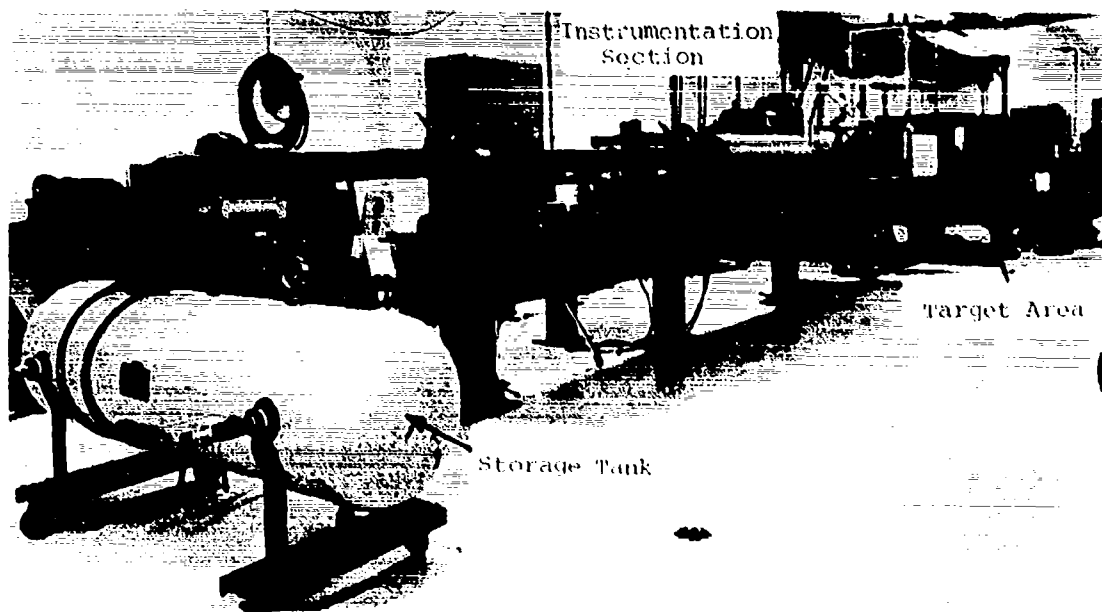


Figure 3. Overall View of the 88.9 mm Gun Range.

The sabot used to carry the bird was an 88.9 mm OD foam plastic cylinder with a 12.7 mm hole drilled in its base. The hole was drilled to assist in the smooth release of the bird and to reduce oscillations of the bird in the free flight after sabot separation. These holes permit the driving pressure to act on the base of the bird itself. Therefore, the bird was both pushed and pulled out of the sabot during the separation process. This sabot is shown in Figure 4.

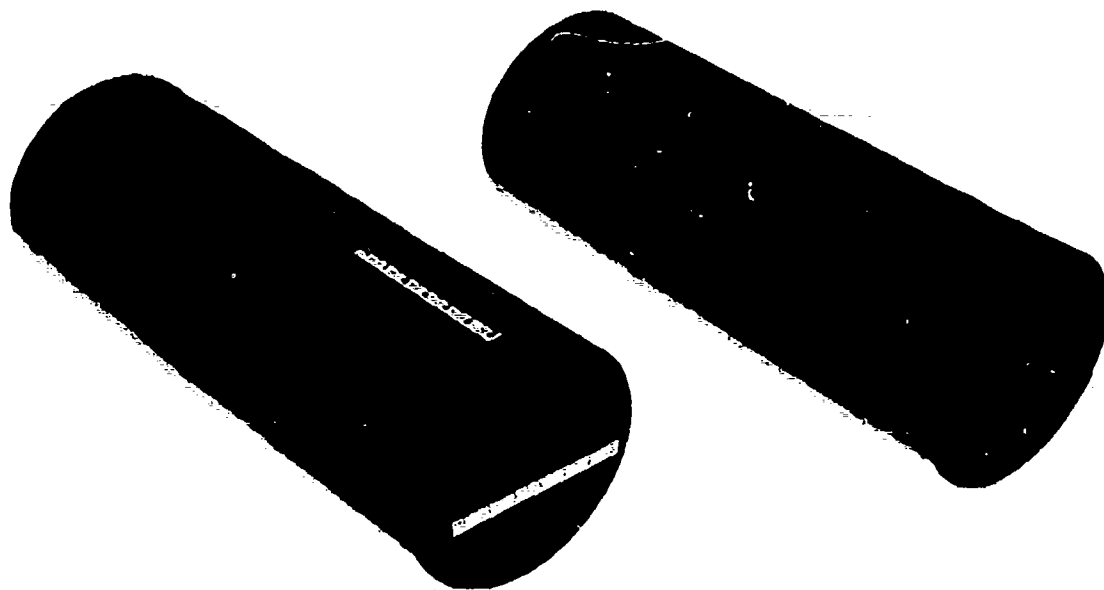


Figure 4. Foam Plastic Sabot Used for Launching Axial Birds.

## 2. TARGET DESCRIPTION

Two different targets were used in this experimental program; a flat rigid steel target plate and flat polycarbonate panels.



The rigid target plate was used to characterize the impact loads exerted by birds with transverse orientations. The target plate was a steel disk, 50.16 cm in diameter and 9.21 cm thick. A series of 0.635 cm holes were drilled along two orthogonal axis of the plate at 2.54 cm intervals. These holes were designed to accept the pressure transducers which were mounted flush with the surface. Depending on the orientation and angle of impact, up to nine transducers were needed to cover the area of impact. The pressure plate is shown in Figure 5.

Flat polycarbonate panels were used to investigate the relative damage potential of birds with different orientations impacting at a 25 degree angle of incidence. The panels were 90 cm long, 60 cm wide, and 0.635 thick. The test panels were rigidly attached to a mounting plate by means of 0.635 cm diameter bolts; the bolts were on a 5.08 cm center-to-center spacing. The mounting plate which was at a 25 degree angle to the bird trajectory, was

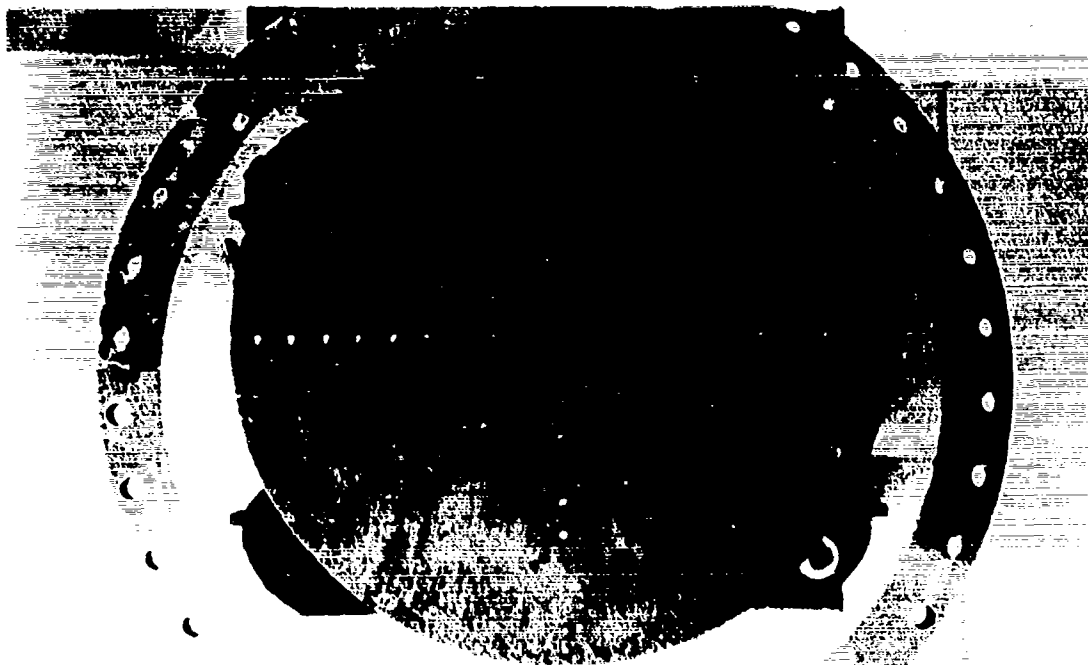


Figure 5. Pressure Plate Mounted for Normal Impacts.

secured to a structural steel support frame. A rigid structural support frame was designed for each gun, and they are shown in Figures 6 and 7. Figure 6 shows the structural support frame used with the 88.9 mm gun and Figure 7 shows the support frame used with the 177.8 mm gun.

### 3. VELOCITY, LOCATION, AND ORIENTATION MEASUREMENT

The velocity of the bird was measured prior to impact using a simple time-of-flight technique. Between the muzzle of the sabot stripper and the target, two helium/neon laser beams were directed across the trajectory. When the bird interrupted the first laser beam, a counter was started. The counter was stopped when the bird interrupted the second laser beam. The distance between the laser beams and the elapsed time were used to calculate the velocity. To increase the accuracy of the velocity measurements and to monitor bird orientation and integrity prior to impact, two orthogonal pulsed x-ray systems were set up at each laser beam station. The resulting radiographs of the bird in flight were used to accurately establish the position of the bird with respect to the laser beams and to monitor the condition and orientation of the bird. This technique proved completely satisfactory for measuring bird velocity; velocities were measured to within one percent. The orientation of the projectile relative to the target was also determined from the orthogonal radiographs. Difficulties in determining the orientation of the bird were encountered in the case of transverse impacts, because the images of the ends of the bird were superposed in the radiograph taken from the x-ray head along the major axis of the bird. Different techniques were tried to eliminate this problem. The best results were obtained by inserting a 1.27 cm long aluminum wire at the center of each end of the bird. Aluminum was chosen because it is soft and does not damage the target (pressure plate or polycarbonate panels). The difference in density between the bird and the aluminum

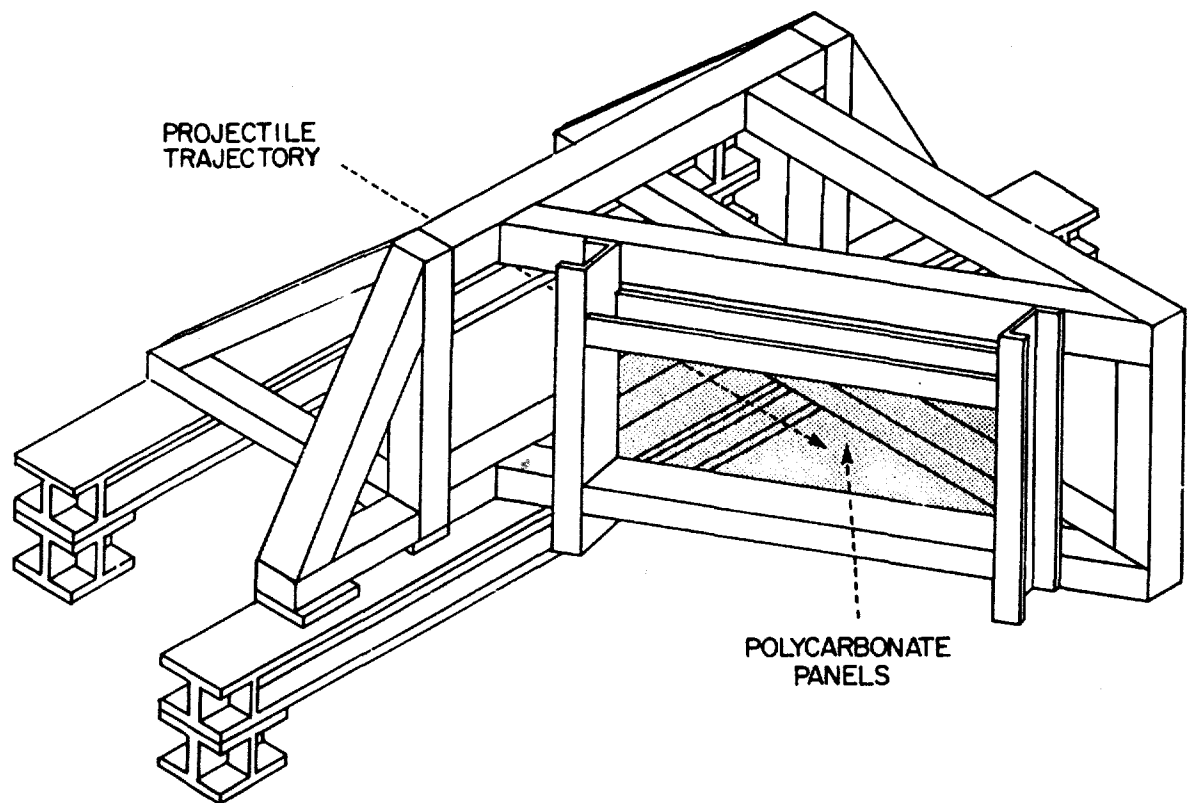


Figure 6. Support Structure and Mounting Frame used with the 88.9 mm Gun.

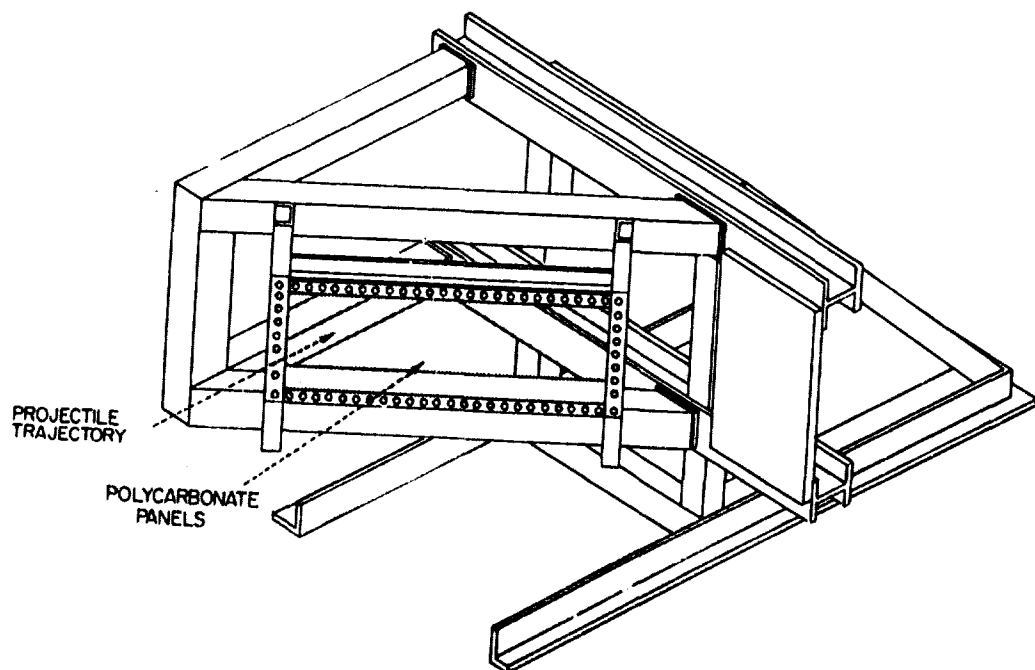


Figure 7. Support Structure and Mounting Frame used with the 177.8 mm Gun.

wire made a clear image on the radiograph, and thereafter orientation was determined to within 0.5 degrees. A typical x-radiograph of the bird with transverse orientation is shown in Figure 8.

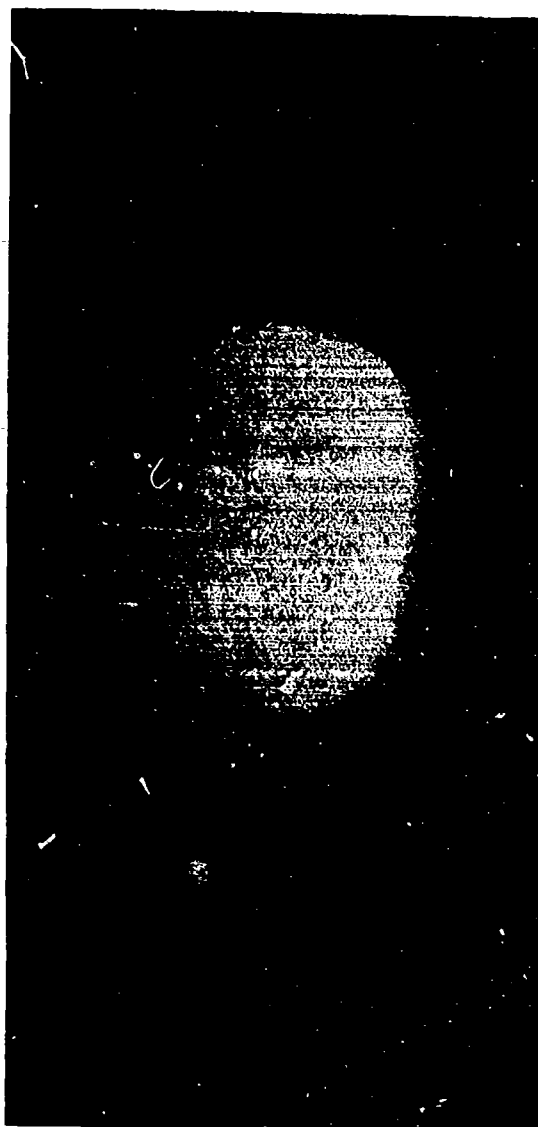
In addition to x-radiograph coverage of the bird in flight, high speed motion picture coverage was also obtained on selected shots. Cameras with framing rates of up to 7,000 f/s were employed for specific investigations of the behavior of the bird and panel during impact.

#### 4. PRESSURE MEASUREMENTS AND RECORDING

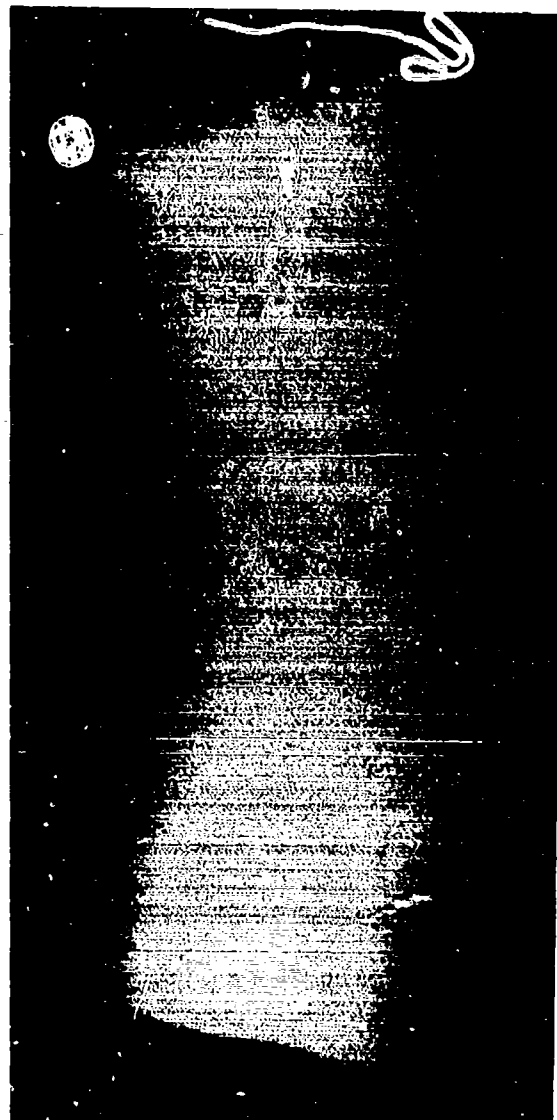
During bird impact the shock pressure can be extremely high, the duration of the impact is relatively short and there can be important pressure excursions. The pressure sensing devices must be capable of measuring and withstanding these high pressures and the pressure sensing and recording equipment must have adequate bandwidth to detect and record important pressure transients.

Piezoelectric quartz pressure transducers were used as the basic sensing devices for these experiments. These transducers have a compact impedance converter physically located in the coaxial line close to the crystal; they have a specified pressure range of 0 to 700 MN/m<sup>2</sup>, and a specified band width from 0 to 80 kHz. Since these transducers are not specifically designed for impact testing, calibration was necessary to verify their operation. A calibration method for the transducers was developed to verify the applicability of the manufacturer's calibration data to the unidirectional axial loads anticipated. The details of these calibration techniques are reported in Reference 1. A device was fabricated to enable the unidirectional axial loads similar to bird/plate impact loads to be applied to the transducer. Then, measurements were taken to determine the response of the transducers. It was concluded

1. Barber, J. P. and J. S. Wilbeck, "The Characterization of Bird Impacts on a Rigid Plate: Part 1," AFFDL-TR-75-5, ADA021142, January 1975.



(a)



(b)

Figure 8. X-radiograph of a 450 g Transversely Oriented Bird Substitute in Free-Flight. (a) from x-ray head along major axis of bird; (b) from x-ray head normal to major axis of bird.

that the transducers provide reliable, accurate pressure data over the range of pressures and frequencies expected. The transducers were mounted flush with the surface of the steel target plate described in paragraph 2.2. Up to nine transducers were simultaneously mounted in the plate on orthogonal axes intersecting at the planned center of impact.

The pressure signals were recorded using an electronic digital memory system. This system uses an analog-to-digital signal converter. The system has a 200 kHz sample rate, and the capability to store 2048 data points in shift registers on each of ten channels. The analog pressure signals were displayed on an oscilloscope, as a function of time, and the time interval of interest determined. Then, digital data over these intervals were recorded on a cassette and were printed out on an electronic data terminal. This technique significantly increased the accuracy and reliability of the data.

## SECTION III

### EXPERIMENTAL RESULTS

Historically, all experimental evaluation of transparency birdstrike resistance have involved axial or end-on impact of the bird. No attempt has ever been made to identify other impact orientations which might prove more severe to the transparency than axial impacts.

Actually, birds strike aircraft transparencies with a random orientation and axial impacts have a low probability of occurrence. Therefore, this program was undertaken to investigate and document the effects of orientation on bird impact loads and on subsequent transparency damage to identify the worst-case orientation and the loads associated with it. The program was divided into two subtasks. The first subtask was designed to characterize the loads exerted by birds striking a rigid flat plate with a transverse orientation, and the second dealt with the relative damage potential of axial and transverse bird impacts on a flat polycarbonate panel.

#### 1. BIRD LOADING STUDIES

A total of 45 test shots were performed to investigate the effects of bird orientation on impact loading. The projectiles used in these tests were 450 g bird substitutes (gelatin with 10 percent porosity). They were right circular cylinders with a length to diameter ratio of approximately two. Projectiles were launched with two different transverse orientations, flat-on (both ends of the bird impact simultaneously) and side-on (the ends of the bird impact at different times for oblique impact angles). The two orientations are shown in Figure 9. Tests were conducted at three impact angles; 90, 45, and 25 degrees and at three velocities; 100, 200, and 300 m/s.

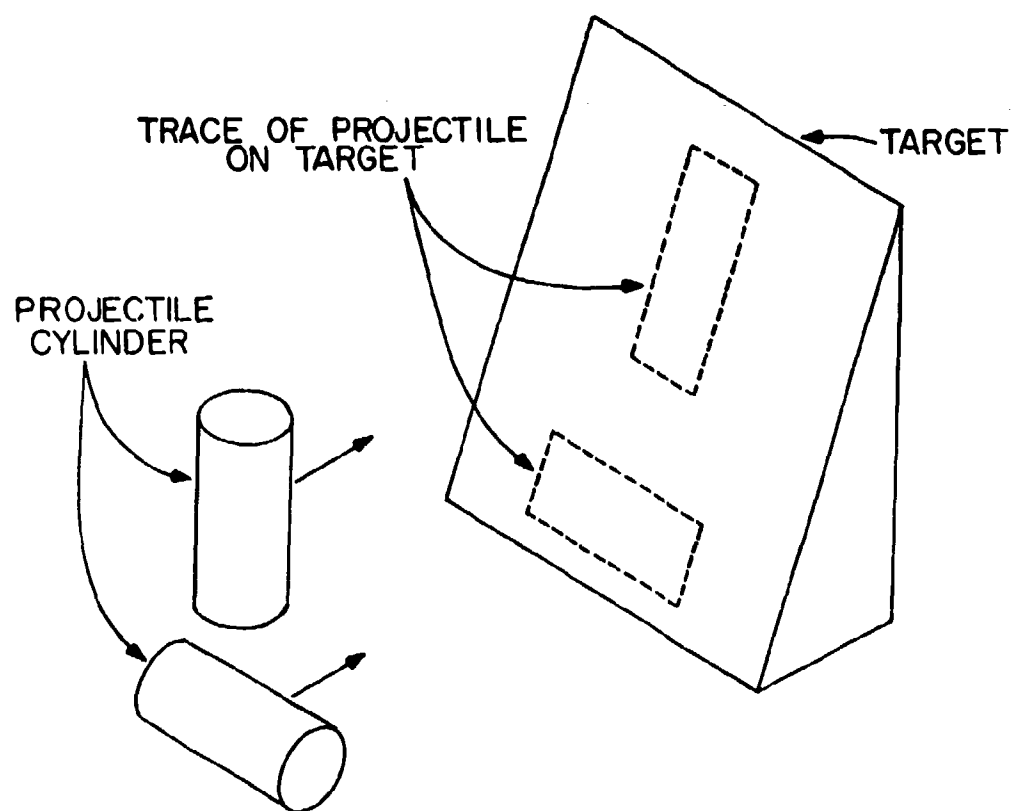


Figure 9. Bird Orientations for Oblique Transverse Impacts. The upper projectile illustrates a side-on impact; the lower projectile illustrates a flat-on impact.



Time varying pressure data were collected using a digital data memory system as described in Section II. From these recorded data, measurements were made to obtain peak pressure and impact duration. The results of these measurements, together with comparisons to theoretical results and measurements from impacts of birds with axial (end-on) orientation reported by Barber in Reference 2 and Challita in Reference 3, are presented in the following sections.

a. Pressure-Time History

It was shown in previous studies reported by Barber in References 1 and 2, by Challita in Reference 3, and by Wilbeck in Reference 4 that birds, independent of their masses, behave like fluids during end-on impacts and the characteristic pressures are the Hugoniot, or impact, pressure and the flow, or stagnation, pressure. Both of these pressures were found to depend only on the impact velocity and the material properties and, since birds of different mass are geometrically similar, pressure distribution scales linearly with bird dimensions.

When birds strike side-on rather than end-on, no region of steady flow pressure was detected for the bird geometries investigated. The initial impact produced the high characteristic (Hugoniot) pressures. These pressures decay as release waves propagate in from the nearest free surface (i.e., the closest edge of the bird). In an end-on impact, the release process

1. Barber, J. P., and Wilbeck, J. S., "The Characterization of Bird Impacts on a Rigid Plate: Part I," AFFDL-TR-75-5 ADA021142, January 1975.
2. Barber, J. P., Taylor, H. R., and Wilbeck, J. S., "Bird Impact Forces and Pressures on Rigid and Compliant Targets," AFFDL-TR-77-60, ADA061-313, May 1978.
3. Challita, A., and Barber, J. P., "The Scaling of Bird Impact Loads," AFFDL-TR-79-3042, June 1979.
4. Wilbeck, J. S., "Impact Behavior of Low Strength Projectiles," AFML-TR-77-134, July 1978.

is over well before the trailing end of the bird reaches the target and steady flow of the bird onto the target occurs. The steady flow is finally terminated when the end of the bird reaches the target. In contrast, the Hugoniot pressure decay process is still continuing as the trailing edge of the bird reaches the target when a bird strikes side-on (for the range of geometries investigated). Accordingly, the shock pressure decays continuously to zero and no pressure plateau indicative of the steady state phase of the impact process is observed. This can be seen in Figures 10 and 11. Figure 10 shows typical pressure traces from normal and oblique impacts of a nominal 450 g right circular cylindrical gelatin projectile with flat-on orientation. Figure 11 shows similar pressure traces from side-on impacts. The points of interest on these tracers are the peak pressure and the impact duration.

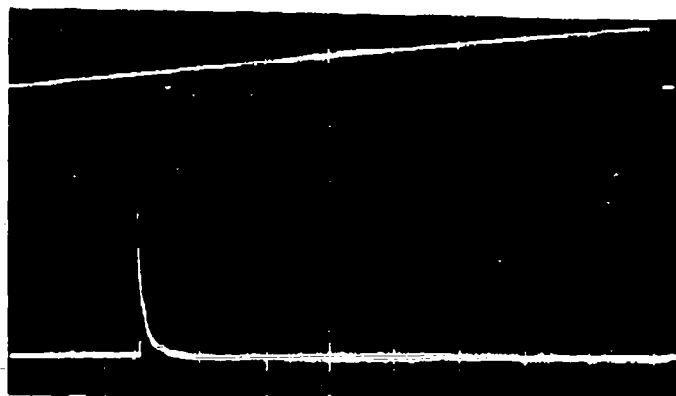
The peak pressure is due to a shock wave formed from the initial impact, and is mainly a function of the normal component of impact velocity and the projectile properties. The impact duration is a function of the effective bird length and the impact velocity.

b. Impact Phases

The axial bird impact on a rigid plate was characterized as a fluid dynamic process and was divided into four phases. The first phase is the initial impact phase in which very high shock pressures are generated between the bird and the target. The release of the shocked material resulted in a decaying pressure during phase two. The shock pressure decays to a steady state pressure which characterizes phase three. During this phase the bird flows steadily onto the plate and is regarded as jet flow. The fourth phase of the impact occurs when the trailing end of the bird approaches the plate and the pressure drops to zero. These phases were discussed in detail in Reference 2 by Barber, and

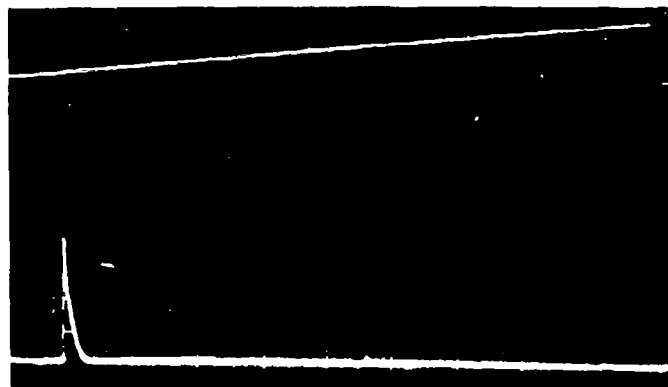
- 
2. Barber, J. P., Taylor, H. R., and Wilbeck, J. S., "Bird Impact Forces and Pressures on Rigid and Compliant Targets," AFFDL-TR-77-60, ADA061-313, May 1978.

$V = 180 \text{ m/s}$   
 $m = 427.6 \text{ g}$   
 $P = 30.34 \text{ MN/m}^2\text{-cm}$   
 $T_s = 920 \text{ } \mu\text{s}$   
 $t = 2000 \text{ } \mu\text{s/cm}$



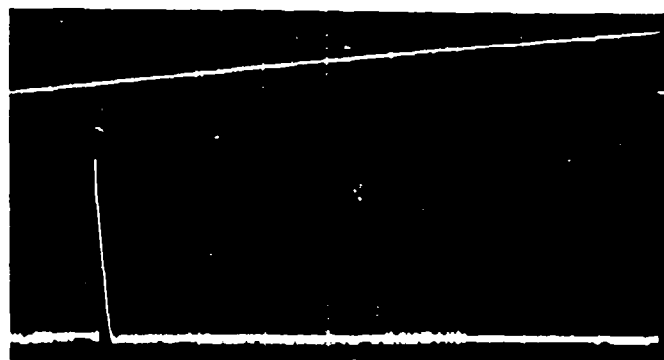
(a)

$V = 179 \text{ m/s}$   
 $m = 428 \text{ g}$   
 $P = 25 \text{ MN/m}^2\text{-cm}$   
 $T_s = 500 \text{ } \mu\text{s}$   
 $t = 2000 \text{ } \mu\text{s/cm}$



(b)

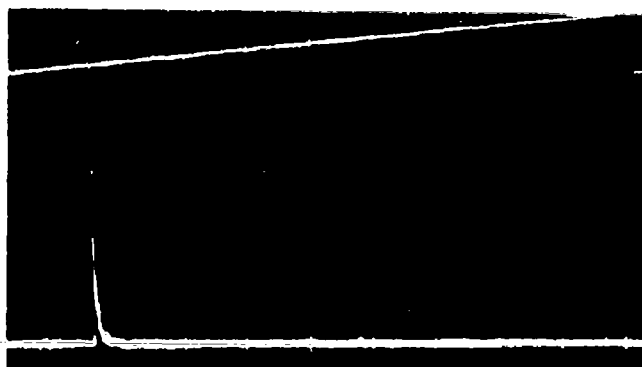
$V = 195 \text{ m/s}$   
 $m = 413.2 \text{ g}$   
 $P = 9.13 \text{ MN/m}^2\text{-cm}$   
 $T_s = 400 \text{ } \mu\text{s}$   
 $t = 2000 \text{ } \mu\text{s/cm}$



(c)

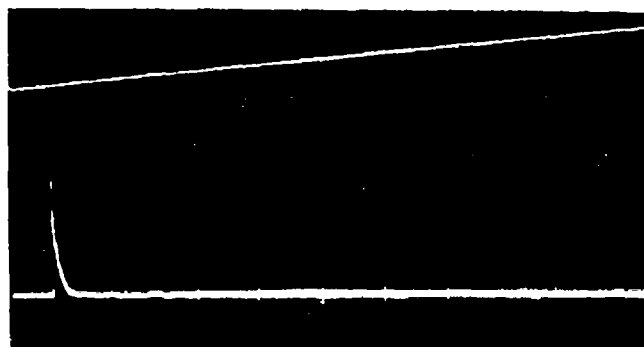
Figure 10. Typical Pressure-Time Record of Nominal 450 g Bird Substitute (gelatin with 10% porosity) from Impacts with Flat-On Orientation. (a) 90° impact, 1" left of center; (b) 45° impact, 2" below center; (c) 25° impact, center transducer.

$V = 203 \text{ m/s}$   
 $m = 422.7 \text{ g}$   
 $P = 91.32 \text{ MN/m}^2\text{-cm}$   
 $T_s = 490 \text{ } \mu\text{s}$   
 $t = 2000 \text{ } \mu\text{s/cm}$



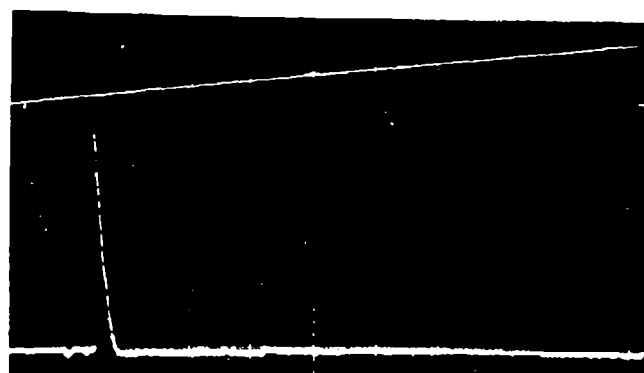
(a)

$V = 299 \text{ m/s}$   
 $m = 431.7 \text{ g}$   
 $P = 49.96 \text{ MN/m}^2\text{-cm}$   
 $T_s = 710 \text{ } \mu\text{s}$   
 $t = 2000 \text{ } \mu\text{s/cm}$



(b)

$V = 302 \text{ m/s}$   
 $m = 417.7 \text{ g}$   
 $P = 6.25 \text{ MN/m}^2\text{-cm}$   
 $T_s = 590 \text{ } \mu\text{s}$   
 $t = 2000 \text{ } \mu\text{s/cm}$



(c)

Figure 11. Typical Pressure-Time Record of Nominal 450 g Bird Substitute (gelatin with 10% porosity) from Impacts with Side-On Orientation. (a) 90° impact, center transducer; (b) 45° impact, 2" below center; (c) 25° impact, 3" below center.

Reference 4 by Wilbeck and were found adequate to describe the impact of a bird with end-on orientation on a rigid plate. As can be seen from the pressure traces in Figures 10 and 11, the impact of a bird with transverse orientation has only two phases; the initial impact pressure phase and the impact pressure decay phase. This is true only for birds with relatively small diameters. If a bird has a diameter large enough to allow the shock wave to reach the center before the impact process is completed, a steady state phase will be seen.

(1) Initial Impact Pressure

During the initial impact, the particles on the front surface of the projectile are instantaneously brought to rest relative to the target face and a shock wave propagates into the projectile. As this shock wave propagates into the projectile, it brings the material behind the shock to rest. The pressure in the compressed region is initially very high and is uniform across the impact area. The edge of the projectile is a free surface and the material near the edge is subjected to a very high stress gradient. This stress gradient causes the material to accelerate radially outward and a release wave is formed and propagates inward. The arrival of this release wave at the center of impact marks the end of the initial impact and the beginning of the decay process. The pressure behind the shock, or the Hugoniot pressure, depends on the projectile density, shock velocity and the impact velocity. The Hugoniot pressure was derived by Wilbeck in Reference 4 and is given by:

$$p_H = \rho V_s V_n \quad (1)$$

where:

- $\rho$  = density of the projectile
- $V_s$  = shock velocity (which is a function of the impact velocity and the density of the material)
- $V_n$  = normal component of the impact velocity.

- 
4. Wilbeck, J. S., "Impact Behavior of Low Strength Projectiles." AFML-TR-77-134, July 1978.

$V_n$  is equal to the impact velocity  $V$  for normal impacts, and equal to  $V \sin \theta$  for oblique impact ( $\theta$  is the impact angle). The shock velocity  $V_s$  corresponding to the normal component of the impact velocity  $V_n$  should be used for oblique impact. Wilbeck in Reference 4 derived the relation between the shock velocity and the impact velocity for gelatin with 10 percent porosity. The initial impact pressures measured for all normal and oblique impact of 450 g gelatin with both transverse orientations (side-on and flat-on) are presented along with the corresponding theoretical Hugoniot in Figures 12, 13, and 14. The measured impact pressures for normal impact of nominal 450 g gelatin with flat-on orientation agree very well with the theoretical Hugoniot. The agreement is better than the experimental results of nominal 1800 g and 3600 g gelatin with end-on orientation, and is as good as the measured pressures for normal impact of nominal 1800 g real birds with end-on orientation reported by Challita in Reference 3. The measured impact pressures for oblique impact for gelatin with transverse orientation were, as expected, lower than the calculated values. This departure from predictions was attributed to the relatively shorter duration of the shock pulse in these impacts, and to the limited bandwidth of the transducers which, apparently, resulted in a significant attenuation of the measured signals. This attenuation was also seen in oblique impacts of birds and bird substitutes with end-on orientation.

## (2) Impact Pressure Decay

At initial impact, a shock begins to propagate into the projectile and a radial release wave propagates in toward the center from the free surface edges of the bird. The decay process starts when the release waves converge at the

- 
3. Challita, A., and J. P. Barber, "The Scaling of Bird Impact Loads," AFSDL-TR-79-3042, June 1979.
  4. Wilbeck, J. S., "Impact Behavior of Low Strength Projectiles," AFML-TR-77-134, July 1978.

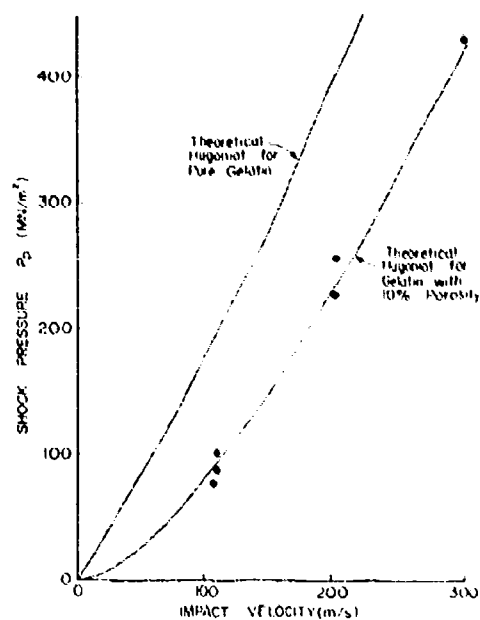


Figure 12. Comparison of Measured Peak Pressures of 450 g Gelatin, Transverse Impacts at 90°, to Theoretical Shock Pressure Curve.

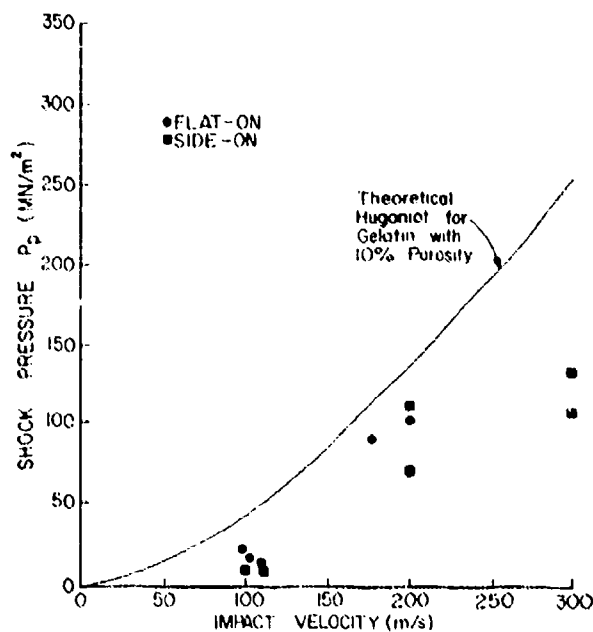


Figure 13. Comparison of Measured Peak Pressures of 450 g Gelatin, Transverse Impacts at 45°, to Theoretical Shock Pressure Curve.

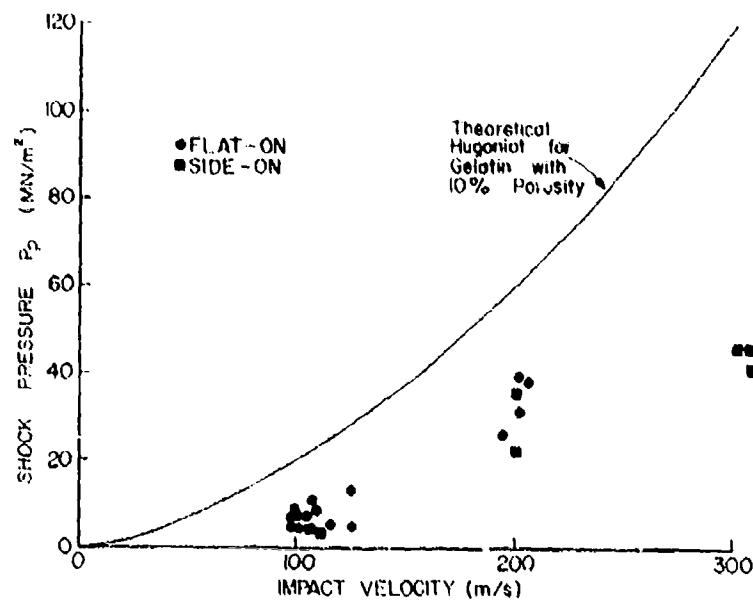


Figure 14. Comparison of Measured Peak Pressures of 450 g Gelatin, Transverse Impacts at 25°, to Theoretical Shock Pressure Curve

center of impact. The release is not instantaneous because of multiple internal reflections and because the release waves are dispersive. However, within a few transit times in the compressed medium, a steady-state flow will be established. In an end-on impact, the release process is over well before the trailing end of the bird reaches the target and steady flow of the bird onto the target occurs during the latter stages of the impact. The steady flow is finally terminated when the end of the bird reaches the target. In contrast, Hugoniot pressure decay is still continuing as the trailing edge of the bird reaches the target when a bird strikes side-on, or flat-on. This can be seen from the pressure traces in Figures 10 and 11 where the shock pressure decays to zero and no pressure plateau indicative of the steady-state phase of impact process is observed. As mentioned before, this is true only for relatively small diameter birds.



c. Impact Duration

The time duration of impact was derived by J. Barber in reference 2. By assuming the bird to be a fluid body, the impact begins when the leading edge of the bird touches the target. The impact continues until the trailing edge reaches the target and there is no further bird material flowing onto the target. Hence, the impact duration,  $T_s$ , was given by:

$$T_s = l/v \quad (2)$$

where:

$l$  = length of the bird

$v$  = impact velocity.

In an oblique impact the effective length of the bird is longer than the "straight" length of the bird,  $l$ . The effective lengths for different bird orientations are shown in Figure 15. For an end-on orientation, the effective length,  $l_{eff}$ , would be given by:

$$l_{eff} = l + d/\tan \theta \quad (3)$$

for a flat-on case  $l_{eff}$  would be:

$$l_{eff} = d/\sin \theta \quad (4)$$

and for a side-on:

$$l_{eff} = d + l/\tan \theta \quad (5)$$

where:

$d$  = diameter of the bird

$l$  = length of the bird

$\theta$  = angle of impact.

- 
2. Barber J. P., H. R. Taylor, and J. S. Wilbeck, "Bird Impact Forces and Pressures on Rigid and Compliant Targets," AFFDL-TR-77-60, ADA061-313, May 1978.

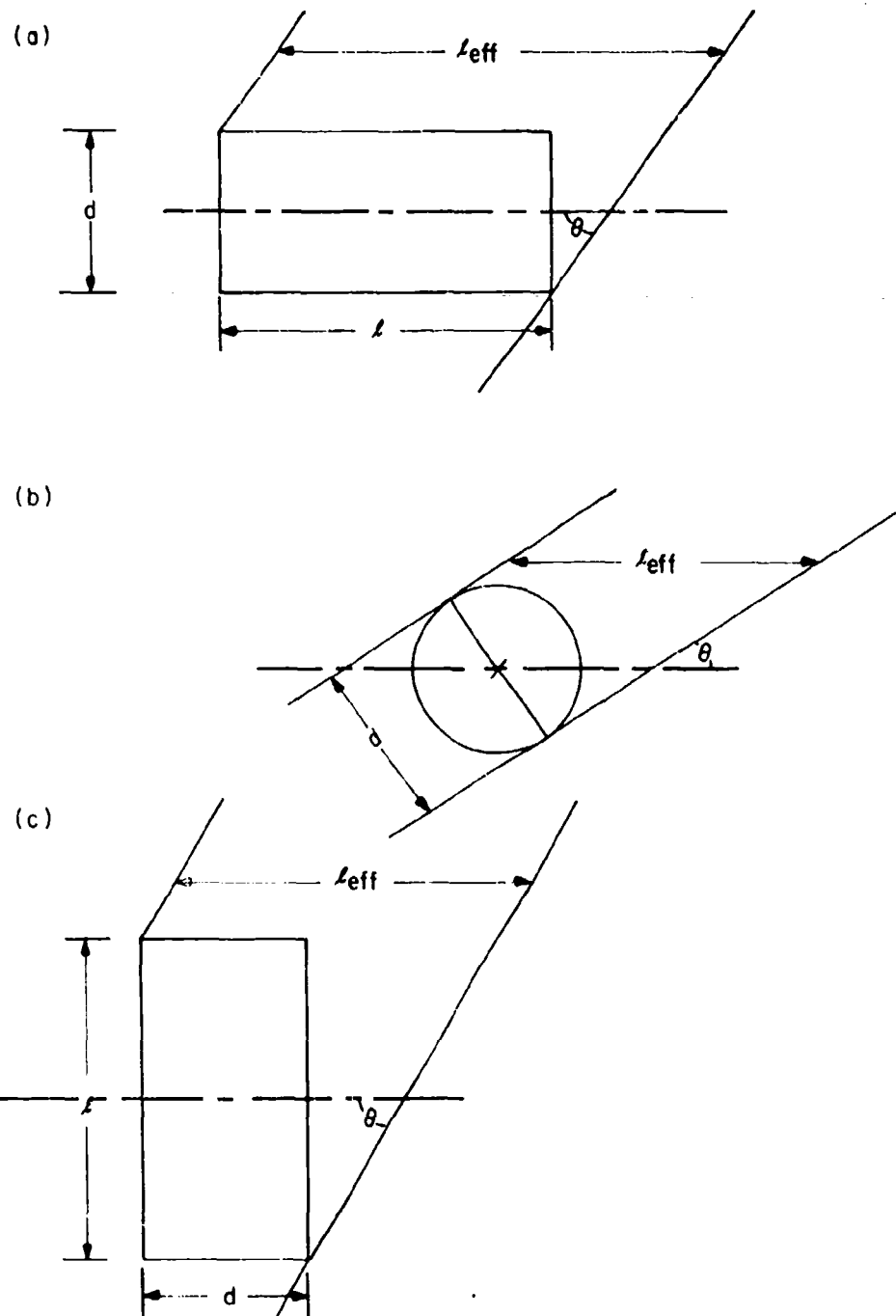


Figure 15. (a) Oblique Impact Effective Bird Length, End-on.  
 (b) Oblique Impact Effective Bird Length, Flat-on.  
 (c) Oblique Impact Effective Bird Length, Side-on.

Theoretically, the "squash-up" time on any transducer is less than the impact duration and greater than a minimum value that depends on the radial distance of the transducer from the center of impact. The "squash-up" time on each transducer was measured for every shot and compared to the theoretical values given by equations 2 through 5. The results agreed very well with the theoretical values for the shots with acceptable deviation from the launched orientation. Deviation from the launched transverse orientation is considered acceptable if both ends of the projectile hit the major axis of the target plate as shown in Figure 16.

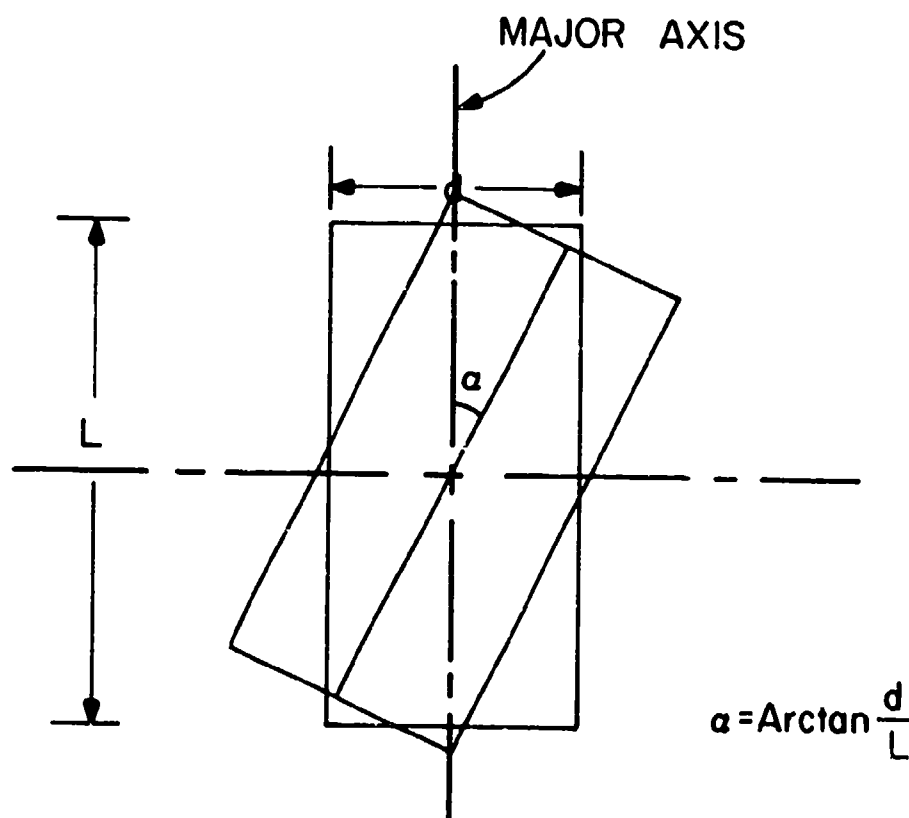


Figure 16. Acceptable Rotation.  $\alpha$  is the maximum allowable rotation.  $\alpha$  is measured in the plane of the target plate.

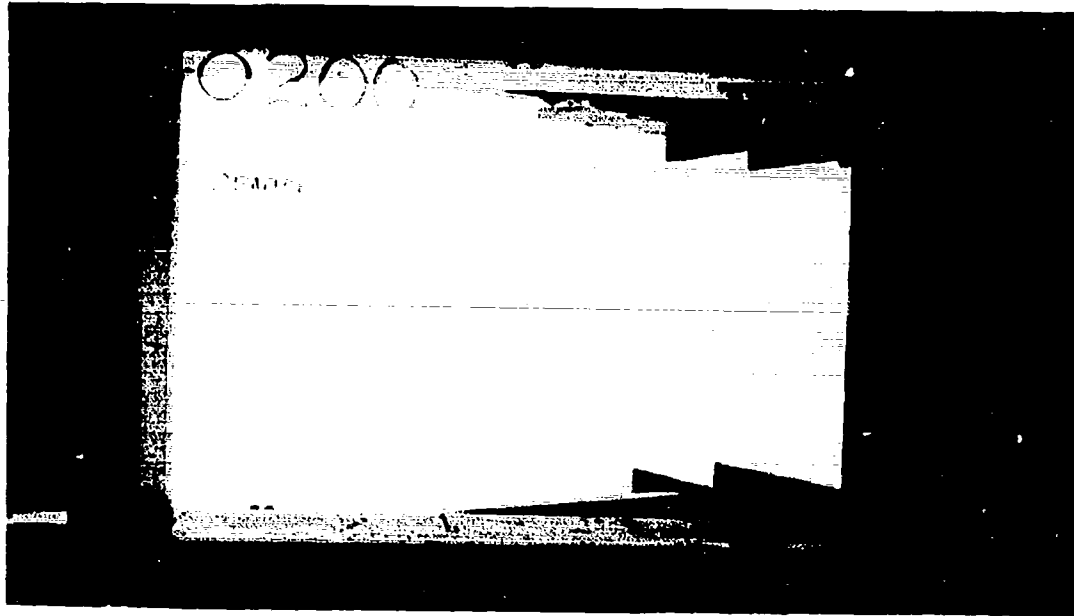


Figure 17. Polycarbonate Panel Bolted to the Structure

## 2. DAMAGE POTENTIAL STUDIES

The objective of this task was to investigate, compare, and document the damage potential of birds as a function of impact orientation and impact location.

A total of 66 shots were conducted in this task. The same projectile geometry and density used in the pressure tests were used. Projectiles were launched with three orientations; axial or end-on, side-on, and flat-on (see Figure 9). They were impacted at a 25 degree angle of incidence onto a nominal 90 cm long, 60 cm wide, and 0.635 cm thick flat polycarbonate panel. The panel was bolted to a relatively rigid support structure as shown in Figure 17. Four impact locations were investigated. They were center panel, down-stream center edge, and up-stream and down-stream corner as shown in Figure 18. These locations were selected to span

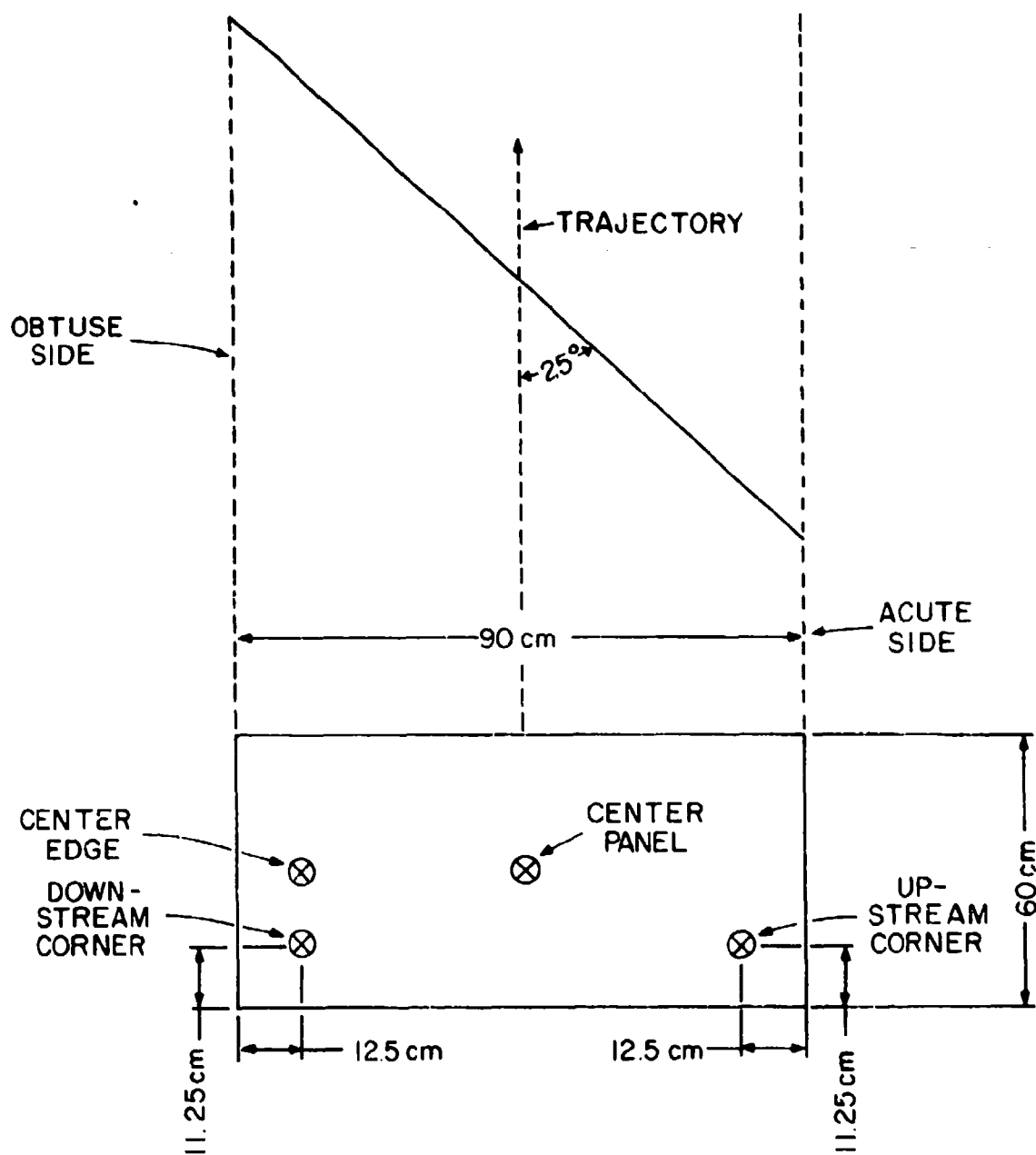


Figure 18. Impact Locations of Bird Substitute onto Polycarbonate Panels.

the range of relatively unconstrained impact (center panel), to constraint on two sides of the impact point (corner impact). The conditions selected also generally correspond to conditions present at locations of interest on typical aircraft transparency systems.

The ballistic limit, or the minimum perforation velocity, was used as the primary criterion for measuring target damage. Secondary criteria such as the length of cracks, volume of plastic pocket, and depth of pocket were used when perforation wasn't achieved. Perforation wasn't achieved for any impacts at the center of the panel and the up-stream corner locations.

The minimum perforation velocity was determined by using a Newtonian iteration search routine. According to this technique, the first shot will be at:

$$V_1 = (V_{\min} + V_{\max})/2 \quad (6)$$

If the target is perforated at  $V_1$ , then the next shot will be at:

$$V_2 = (V_1 + V_{\min})/2 \quad (7)$$

otherwise

$$V_2 = (V_1 + V_{\max})/2 \quad (8)$$

If both  $V_1$  and  $V_2$  resulted in perforation, then:

$$V_3 = (V_2 + V_{\min})/2 \quad (9)$$

This technique was not used throughout the program; it was only used at the beginning, since no past experience was available. Using this technique, a maximum of five shots was sufficient to determine the perforation velocity to within 4 m/sec.  $V_{\min}$  and  $V_{\max}$  were 100 and 300 m/sec respectively.

a. Factors Affecting Damage

As a preface to discussing the results of this study it is pertinent to address, in a cursory manner, the factors

affecting the threshold of fracture in transparent crew enclosure panels. First, it should be pointed out that the dynamic response of a structure to impact loading is a characteristic of the total structural system and cannot generally be evaluated in terms of the individual structural components isolated from the total system. Thus, evaluating birdstrike damage in terms of impact location and bird orientation could be expected to show variation from one structural system to another.

Design details are also an important consideration in determining structural integrity. This is especially important for bird impact where the loading is rapid and the strain rates are high. Improper matching of transparency/support structure stiffness, poor edge design, and improper fastening techniques can all lead to premature failure.

These considerations might tend to preclude achievement of the task objective. However, previous experience with the birdstrike testing of flat panels and full scale flight hardware has served to identify the most critical impact locations and the failure modes associated with good design practice. Furthermore the experiment was designed to eliminate failure initiated at the bolted attachment and to permit large plastic deformations prior to rupture. Thus, even though the design tested is by no means an optimum structural system, it is believed that the results can provide some meaningful guidance with respect to the effects of bird orientation at impact.

b. Summary of Results

A summary of the tests conducted during this experimental program is presented in Table 1. Bird orientation, impact location, impact velocity, and a description of the resultant target damage are included in Table 1. Photographs of the panels impacted at velocities above and below the threshold velocity for all bird orientations and impact locations are presented in the Appendix.

TABLE 1  
TEST SUMMARY

Shot Number	Impact Location	Bird Orientation	Velocity (m/s)	Panel Post Test Condition
4.0057	Center panel	End-on	232	Panel broke; shattered. This panel was scratched badly before impact.
4.0058	"	"	223	Didn't break; small dent near obtuse edge; some yielding along top and obtuse edges.
4.0059	"	"	229	Didn't break; small dent near obtuse edge; some yielding along top and obtuse edges.
4.0060	"	"	237	Didn't break; small dent near obtuse edge; some yielding along top and obtuse edges.
4.0061	Center edge 5" from obtuse	"	220	Panel broke; 7.7-inch long tear near the obtuse edge; some yielding along top and obtuse edges.
4.0062	"	"	222	Panel broke; 8-inch long tear near the obtuse edge; some yielding near top and obtuse edges.
4.0063*	"	"	204	Didn't break; 1 inch deep ridge near the obtuse edge; some yielding along top and obtuse edges.
4.0064*	"	"	212	Panel broke; 6.7-inch long tear near the obtuse edge; some yielding along top and obtuse edges.
4.0065*	Center panel	"	290	Didn't break; 7.6 inch long, 7 inch wide, 1.2 inch deep pocket; hump at center of impact; yielding along top and obtuse edges; small dent near obtuse edge.
4.0066	Center panel	"	305	Didn't break; 12.6 inch long, 10.8 inch wide, 2.3 inch deep pocket; hump at center of impact; yielding along top and obtuse edges.
4.0067*	"	"	307	Didn't break; 13 inch long, 12 inch wide, 2.4 inch deep pocket; hump at center of impact; yielding along top and obtuse edges.
4.0068	Down-stream corner 5" from obtuse 5-3/4" from bottom	"	204	Panel broke; 7.6 inch long tear near the obtuse edge; yielding along bottom and obtuse edges.
4.0069	"	"	189	Panel broke; 6.8 inch long tear near the obtuse edge; yielding along bottom and obtuse edges.



TABLE 1 (CONTINUED)

Shot Number	Impact Location	Fire Orientation	Velocity ( /s)	Panel Post Test Condition
4.0070	Down-stream Corner	End-on	153	Didn't break; small dent near the obtuse edges; some yielding along bottom and obtuse edges.
4.0072*	"	"	171	Didn't break; 0.5 inch deep dent near the obtuse edge; yielding along bottom and obtuse edges.
4.0073*	"	"	175	Panel broke; 6.3 inch long tear near the obtuse edge; yielding along bottom and obtuse edges.
4.0074	Up-stream corner	"	205	Didn't break; no visible damage or deformation; some yielding along bottom and obtuse edges.
5 4.0075	5" from acute 5-3/4" from bottom	"	240	Didn't break; no visible damage or deformation; some yielding along top, bottom, and obtuse edges.
4.0076*	"	"	313	Didn't break; 13.85 inch long 10.6 inch wide, 2 inch deep pocket; small hump in center of pocket; yielding along top, bottom, and obtuse edges.
4.0077*	"	"	303	Didn't break; 12 inch long 7.4 inch wide, 1.9 inch deep pocket; small hump in center of pocket; yielding along top, bottom, and obtuse edges.
5.0142	Center edge 5" from obtuse	Flat-on	142	Panel broke; long tear near the obtuse edge.
5.0143	"	"	136	Panel broke; long tear near the obtuse edge.
ON RANGE 5 THE FRAME SUPPORTING THE PANELS WAS ROTATED 180 DEGREES; THE EDGE WAS VERY SHARP; IT WAS ROUNDED AFTER SHOT NO. 5.0143.				
5.0144	Center Edge 5" from obtuse	Flat-on	137	Didn't break; small dent near the obtuse edge; yielding along top, and obtuse edges.
5.0145	"	"	206	Panel broke; 8.5 inch long tear near the obtuse edge; yielding along top, bottom, and obtuse edges.

TABLE 1 (CONTINUED)

Shot Number	Impact Location	Bird Orientation	Velocity (m/s)	Panel Post Test Condition
5.0146	Center edge 5" from obtuse	Flat-on ↓	188	Didn't break; 0.4 inch deep dent near obtuse edge; yielding along top, bottom, and obtuse edges.
5.0147*	"	"	202	Didn't break; 0.64 inch deep dent near obtuse edge; yielding along top, bottom, and obtuse edges.
5.0148	"	"	197	Didn't break; 0.5 inch deep dent near obtuse edge; yielding along top, bottom, and obtuse edges.
5.0149*	"	"	206	Panel broke; 7 inch long tear near the obtuse edge; yielding along top, bottom, and obtuse edges.
5.0150*	Center Panel	"	297	Didn't break; 9.8 inch long, 8 inch wide, 1.2 inch deep pocket; hump in center of pocket; yielding along top, bottom and obtuse edges; small dent near obtuse edge.
5.0151*	Center Panel	"	307	Didn't break; 8 inch long, 9.2 inch wide, 1.4 inch deep pocket; hump in pocket; yielding along top, bottom, and obtuse edges; small dent near obtuse edge.
5.0152*	"	"	336	Didn't break; 11.2 inch long 8 inch wide, 1.9 inch deep pocket; hump in pocket; yielding along top, bottom, and obtuse edges; small dent near obtuse edge.
5.0153	"	"	234	Didn't break; small hump near center of impact; small dent near obtuse edge; yielding along top, bottom, and obtuse edges.
5.0154	"	Side-on ↔	232	Didn't break; small dent near obtuse edge; yielding along top, bottom, and obtuse edges.
5.0155*	"	"	292	Didn't break; 11.2 inch long, 5.9 inch wide, 0.4 inch deep pocket; yielding along top, bottom, and obtuse edges; small dent near obtuse edge.
5.0156	"	"	305	Didn't break; 12 inch long, 6 inch wide, 0.4 inch deep pocket; yielding along top, bottom, and obtuse edges; small dent near obtuse edge.
5.0157*	"	"	333	Didn't break; 14 inch long, 16 inch wide, 0.8 inch deep pocket; yielding along top, bottom, and obtuse edges; 0.6 inch deep dent near obtuse edge.

TABLE 1 (CONTINUED)

Shot Number	Impact Location	Bird Orientation	Velocity (m/s)	Panel Post Test Condition
5.0158*	Center edge 5" from obtuse	Side-on ↔	210	Didn't break; 0.8 inch deep dent near the obtuse edge; yielding along top, bottom, and obtuse edges.
5.0159	"	"	225	Panel broke; 6.2 inch long tear near obtuse edge; yielding along top, bottom, and obtuse edges.
5.0160*	"	"	212	Panel broke; 7 inch long tear near obtuse edge; yielding along top, bottom, and obtuse edges.
5.0161	"	"	212	Didn't break; 1 inch deep dent near obtuse edge; yielding along top, bottom, and obtuse edge.
5.0162*	Center edge 7-3/4" from obtuse	"	210	Didn't break; 0.8 inch deep dent near the obtuse edge; yielding along top, bottom, and obtuse edges.
5.0163	"	"	209	Didn't break; 0.8 inch deep dent near the obtuse edge; yielding along top, bottom, and obtuse edges.
5.0164*	"	"	212	Panel broke; 7.3 inch long tear near the obtuse edge; yielding along top, bottom, and obtuse edges.
5.0165	Down-stream Corner 5" from obtuse 5-3/4" from top	Flat-on ↑	180	Didn't break; 0.8 inch deep dent near the obtuse edge; yielding along top and obtuse edges.
5.0166*	"	"	121	Didn't break; 0.6 inch deep dent near the obtuse edge; yielding along top and bottom edges.
5.0167*	"	"	182	Panel broke; 6.8 inch long tear near the obtuse edge; yielding along top and obtuse edges.
5.0168	"	Side-on ↔	171	Didn't break; dent near the obtuse edge; yielding along top and obtuse edges.
5.0169	"	"	187	Didn't break; dent near the obtuse edge; yielding along top and obtuse edges.
5.0170	"	"	194	Didn't break; dent near the obtuse edge; yielding along top and obtuse edges.

TABLE 1 (CONTINUED)

Shot Number	Impact Location	Bird Orientation	Velocity (m/s)	Panel Post Test Condition
5.0171	Down-stream Corner 5" from obtuse 5-3/4" from top	Side-on ↔	198	Didn't break; dent near the obtuse edge; yielding along top and obtuse edges.
5.0172	"	"	206	Didn't break; dent near the obtuse edge; yielding along top and obtuse edges.
5.0173	"	"	210	Didn't break; dent near the obtuse edge; yielding along top and obtuse edges.
5.0174	"	"	219	Didn't break; dent near the obtuse edge; yielding along top and obtuse edges.
5.0175*	"	"	237	Panel broke; 7.4 inch long tear near the obtuse edge; yielding along top and obtuse edges.
5.0176	"	"	229	Didn't break; dent near the obtuse edge; yielding along top and obtuse edges.
5.0177*	"	"	232	Didn't break; 1.4 inch deep dent near the obtuse edge; yielding along top and obtuse edges.
5.0178*	Up-stream Corner 5" from acute 5-3/4" from top	Flat-on ↑	350	Didn't break; 13.4 inch long, 11.5 inch wide, 1.8 inch deep pocket; small hump in center of pocket; yielding along top, bottom, and obtuse edges.
5.0179*	"	"	335	Didn't break; 11.5 inch long, 11.4 inch wide, 1.7 inch deep pocket; small hump near center of pocket; yielding along top, bottom, and obtuse edges.
5.0180	"	"	228	Didn't break; 9.7 inch long, 8.8 inch wide, 2.1 inch deep pocket; small hump near center of impact; yielding along top, bottom, and obtuse edges.
5.0181*	"	"	305	Didn't break; 10.8 inch long, 9.2 inch wide, 1.5 inch deep pocket; small hump at center of impact; yielding along top, bottom, and obtuse edges.

TABLE 1 (CONCLUDED)

Shot Number	Impact Location	Bird Orientation	Velocity (m/s)	Panel Post Test Condition
5.0182	Up-stream Corner 5" from acute 5-3/4" from top	Flat-on ↑	225	Didn't break; no apparent damage or deformation; yielding along top and obtuse edges.
5.0183	"	Side-on ↔	231	Didn't break; small dent near obtuse edge; yielding along top and obtuse edges.
5.0184*	"	"	306	Didn't break; 0.1 inch deep hump at center of impact; yielding along top and obtuse edges.
5.0185	"	"	296	Didn't break; shallow hump at center of impact; yielding along top, and obtuse edges.
5.0186	"	"	331	Didn't break; 0.2 inch deep hump at center of impact, yielding along top and obtuse edges.

\* Front and end view of the panels after impact is shown in Appendix A.

Projectiles used to conduct these shots were right circular gelatin cylinders with L/D ratio equal to 2, they were 5.2 inches long.

At the down-stream center edge location the perforation velocity was found to equal  $208 \pm 4$  m/s for end-on,  $204 \pm 2$  m/s for flat-on, and  $212 \pm 1$  m/s for side-on impact. At the down-stream corner, the perforation velocities were  $173 \pm 2$  m/s for end-on,  $184 \pm 3$  m/s for flat-on, and  $234 \pm 2$  m/s for side-on impacts.

Perforation was not achieved at either the center panel location or the up-stream corner location. Examination of center panel shot numbers 4.0067, 5.0151, and 5.0156 (which were at approximately the same velocity) reveals that, in terms of plastic deformation, end-on was the most damaging orientation and side-on was the least damaging. Similarly, examination of up-stream corner shot numbers 4.0076, 5.0181, and 5.0184 (which were at approximately the same velocity) indicates that end-on was the most damaging orientation and side-on was the least damaging.

These results indicate that the side-on impact is the least critical of the three orientations investigated. The same results could be deduced from Figure 9, since both the loaded area and the duration of the impact event increase as the angle of incidence decreases from normal impact. This could be expected to spread the load out and produce significant strains in a larger volume of material with a corresponding reduction in the peak strains.

In terms of the birdstrike testing of full scale flight hardware this result suggests that a significant pitch angle during attempted end-on impact would decrease the criticality of the strike. Further, it would be expected that a negative pitch angle (front of bird down) would be less critical than a positive pitch angle. This is true because as the positive pitch angle approaches the angle on the impacted transparency the impact condition will more closely simulate the flat-on condition. When the pitch angle on the bird equals the angle of the transparency

instantaneous contact will take place over the full length of the bird (assuming that the bird is a right circular cylinder).

Considering all locations it appears that the end-on orientation is slightly more critical than the flat-on orientation for the panel/support structure system tested. The structural system design and the failure mode could affect the critical bird orientation as a function of impact location (Reference discussion in Paragraph 3.2.1) and variation in bird load pressure profiles with respect to angle of incidence and bird orientation. However, based on the limited studies conducted on this program, the use of end-on impact for conducting full scale birdstrike qualification tests seem to be justified.

It is important to stress the importance of controlling the bird orientation at impact during full scale developmental and qualification testing. The kinetic energy of the bird with end-on orientation required to fail the panel at the downstream corner was approximately half the energy required for the bird with side-on orientation. Therefore, measures should be taken at all bird-impact test facilities to account more carefully for the effects of bird orientation at impact.

## SECTION IV

### CONCLUSIONS AND RECOMMENDATIONS

The following conclusions are based on the results of this experimental program.

- 1) Of the three orientations tested (end-on, flat-on, and side-on) side-on was the least critical.
- 2) The end-on orientation appears to be as critical or more critical than any other orientation.
- 3) For a particular design configuration and impact location it is conceivable that the flat-on orientation could be most critical.
- 4) During end-on birdstrike testing pitch and/or yaw of the bird would tend to decrease critically.
- 5) For the bird geometries tested the load-time history exhibited no steady state flow conditions for the transverse bird orientations.
- 6) The duration of the loading can be expressed in terms of an effective length for all bird orientations investigated.

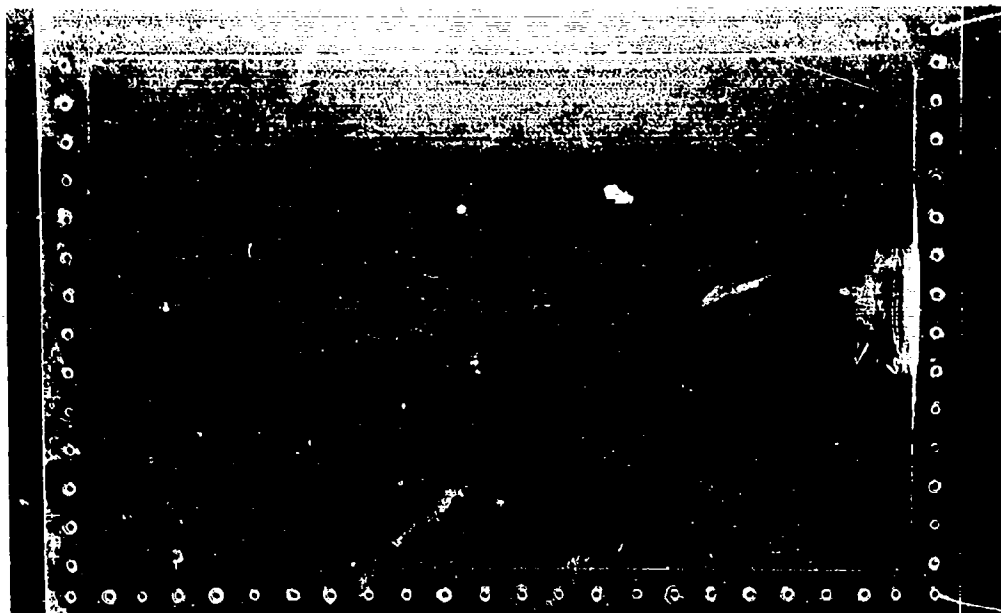
It is recommended that

- 1) Full scale birdstrike developmental and qualification testing continue to be conducted with end-on orientation.
- 2) Bird orientation must be controlled to insure that significant pitch and yaw are not present at the instant of impact.



APPENDIX  
PHOTOGRAPHS OF DAMAGED PANELS

a)



b)

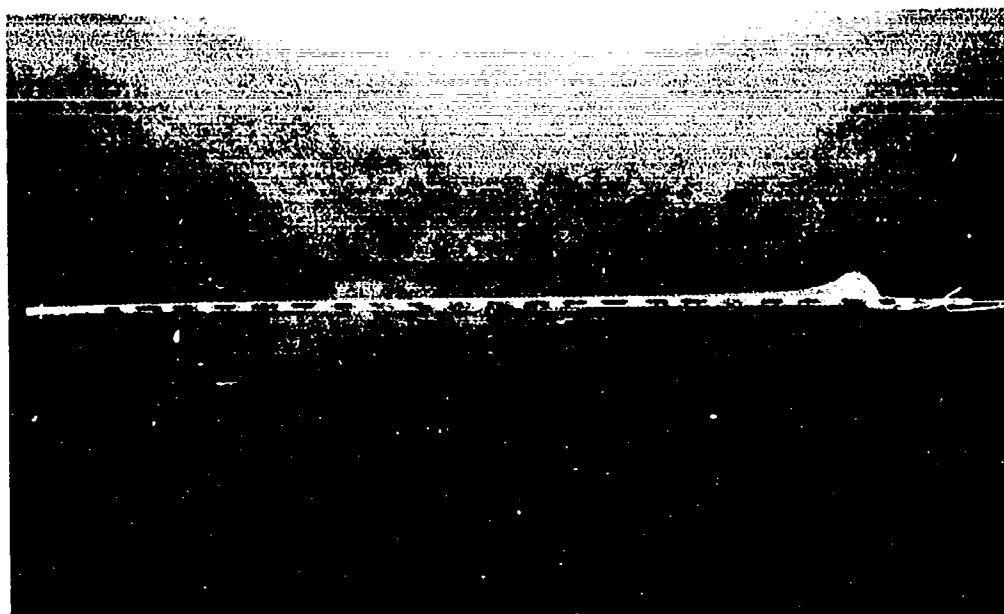


Figure A-1. Shot No. 4-0063; Panel impacted at the center edge; one-pound gelatin launched with an axial orientation at 204 m/s. a) front view; b) end view

a)

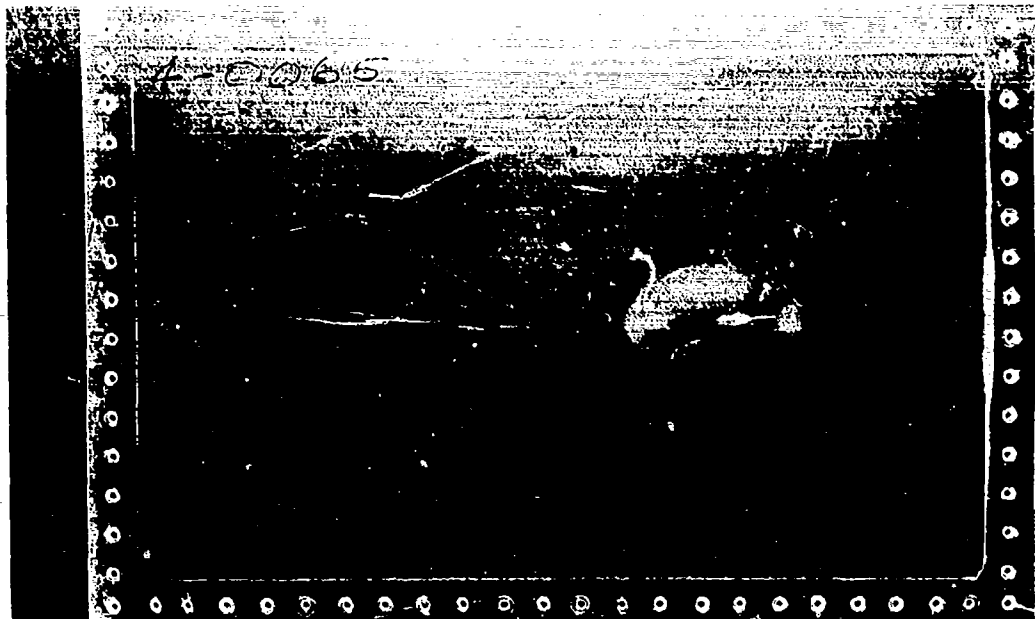


b)



Figure A-2. Shot No. 4-0064; Panel impacted at the center edge; one-pound gelatin launched with an axial orientation at 212 m/s. a) front view; b) end view

a)



b)

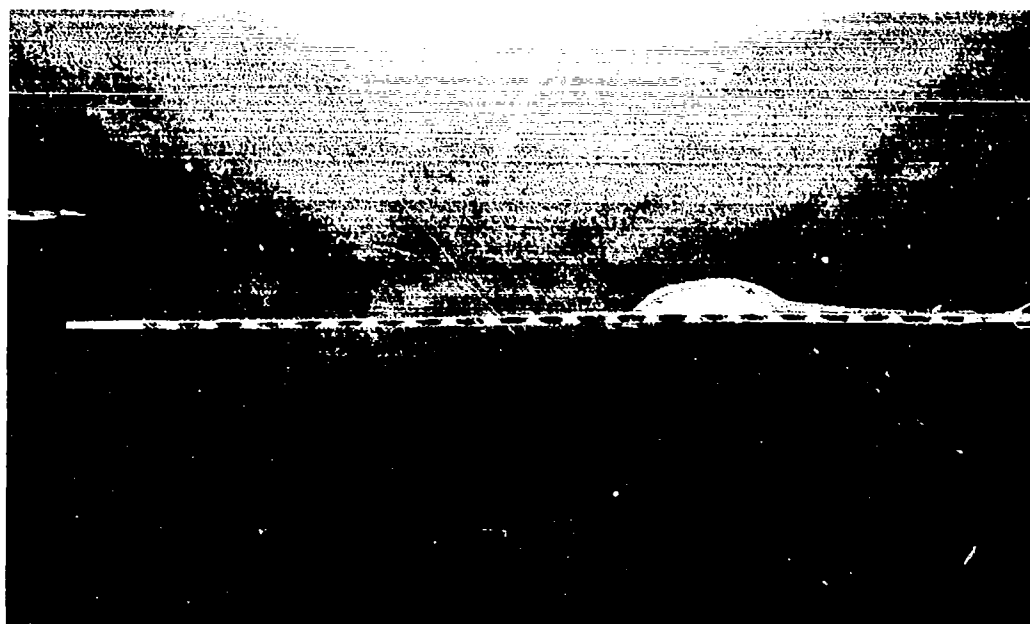
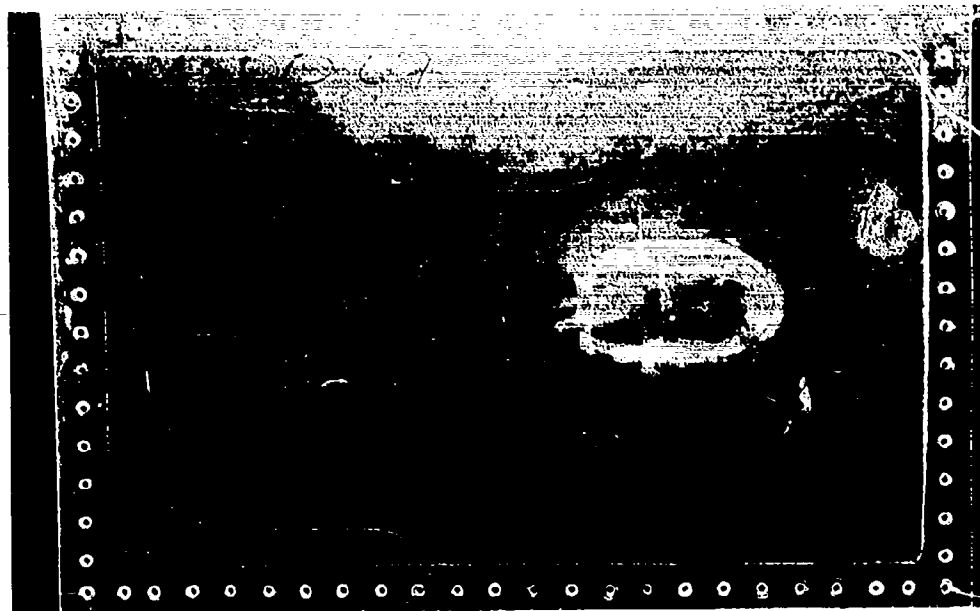


Figure A-3. Shot No. 4-0065; Panel impacted at the center panel; one-pound gelatin launched with an axial orientation at 290 m/s. a) front view; b) end view

a)

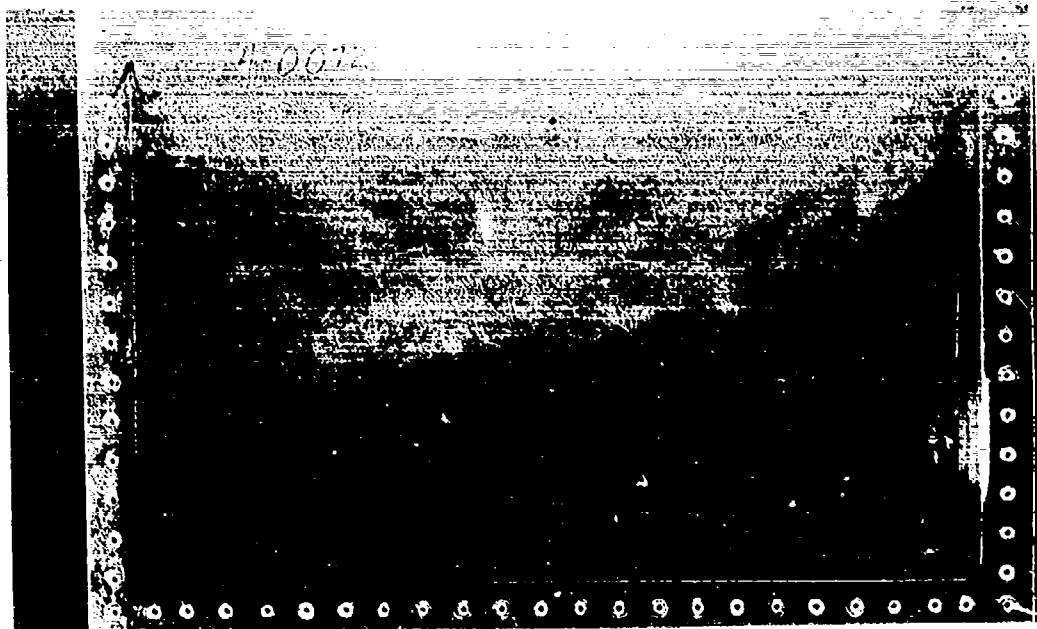


b)



Figure A-4. Shot No. 4-0067; Panel impacted at the center panel; one-pound gelatin launched with an axial orientation at 307 m/s. a) front view; b) end view

a)

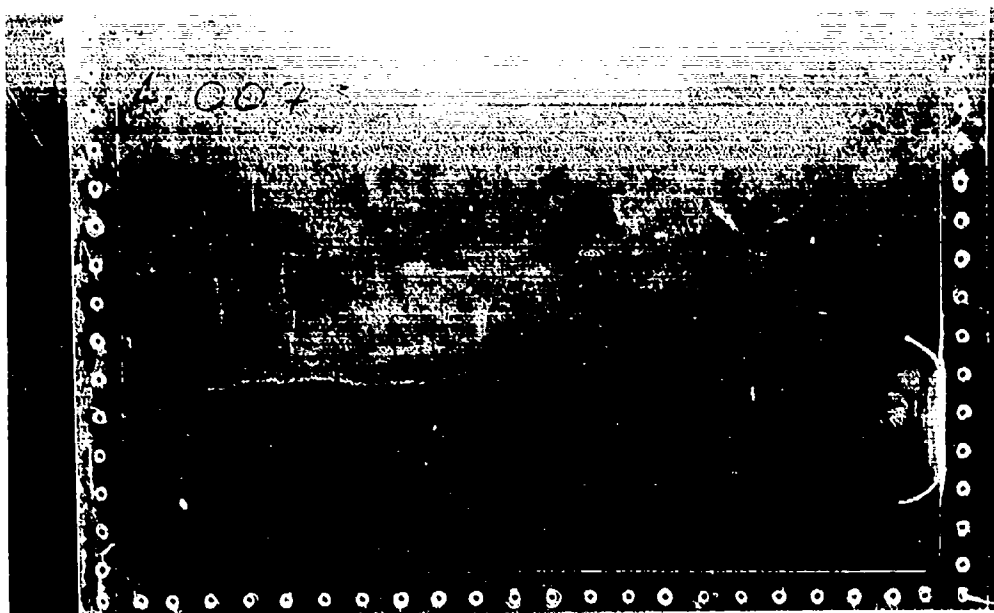


b)



Figure A-5. Shot No. 4-0072; Panel impacted at the down-stream corner; one-pound gelatin launched with an axial orientation at 171 m/s. a) front view; b) end view

a)



b)

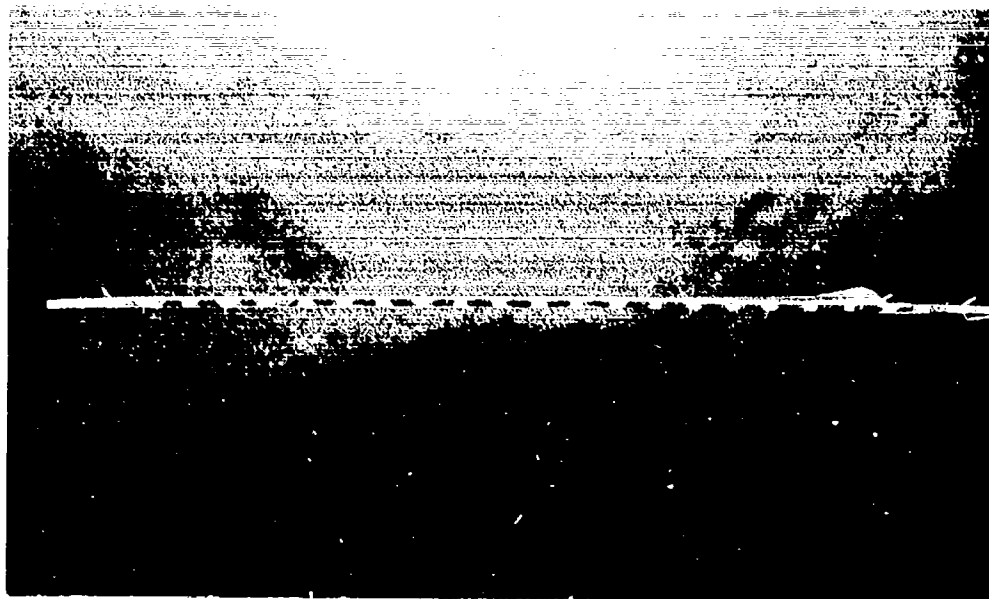
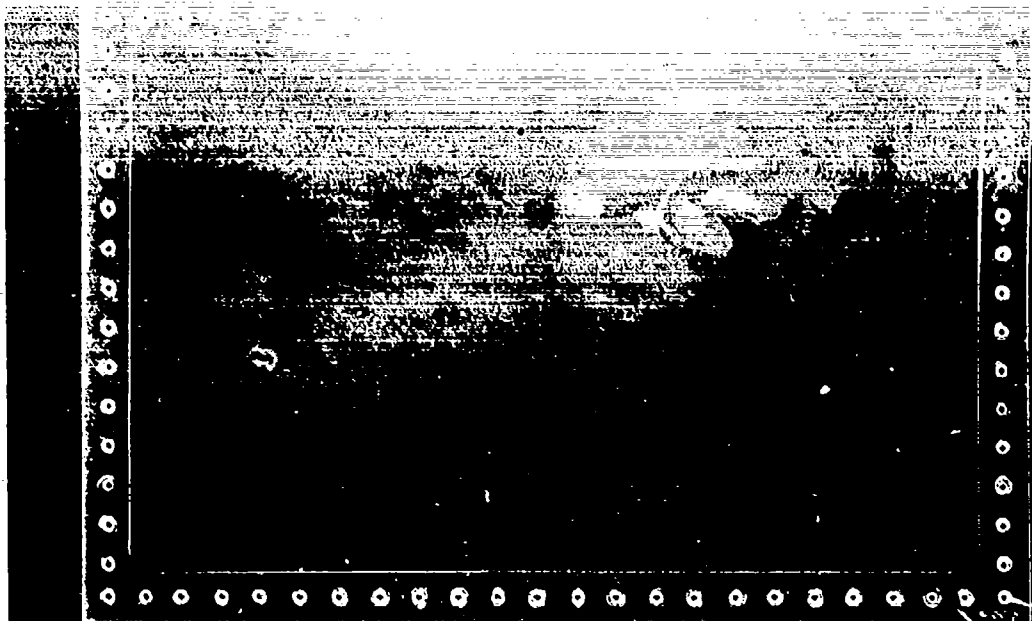


Figure A-6. Shot No. 4-0073; Panel impacted at the down-stream corner; one-pound gelatin launched with an axial orientation at 175 m/s. a) front view; b) end view

a)



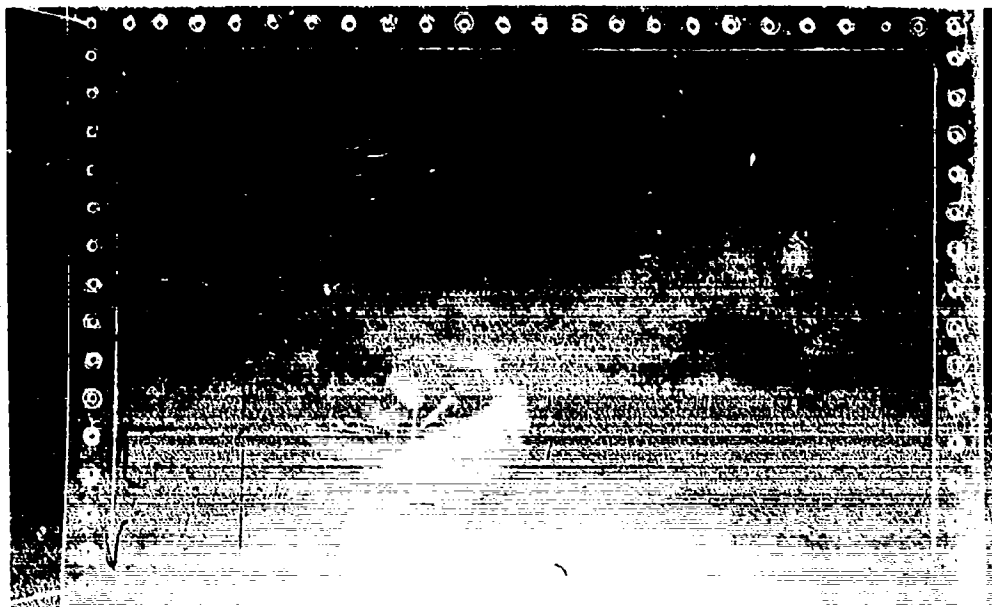
b)



Figure A-7. Shot No. 4-0076; Panel impacted at the up-stream corner; one-pound gelatin launched with an axial orientation at 313 m/s. a) front view; b) end view



a)

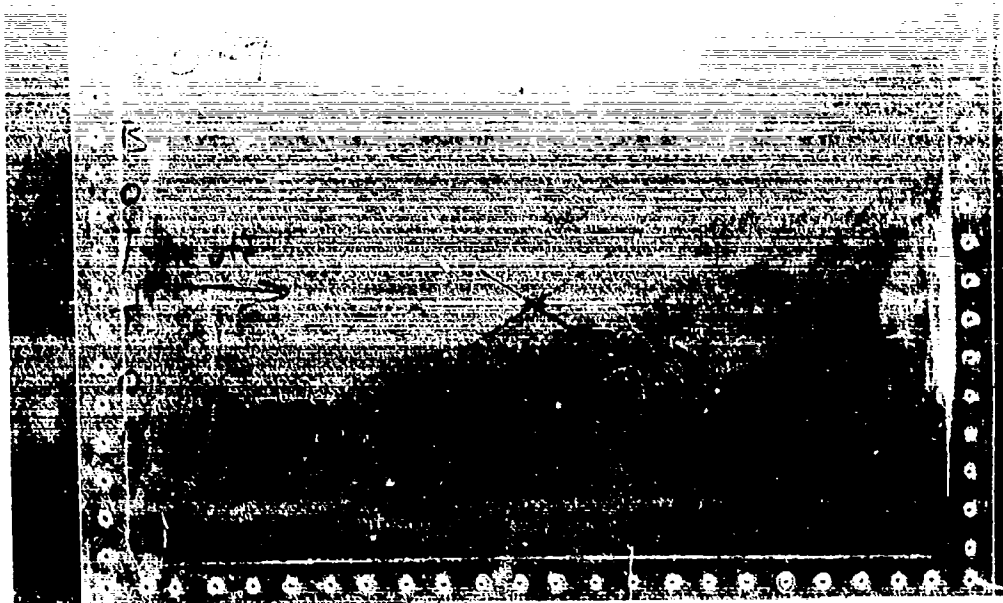


b)



Figure A-8. Shot No. 4-0077; Panel impacted at the up-stream corner; one-pound gelatin launched with an axial orientation at 303 m/s. a) front view; b) end view

a)



b)

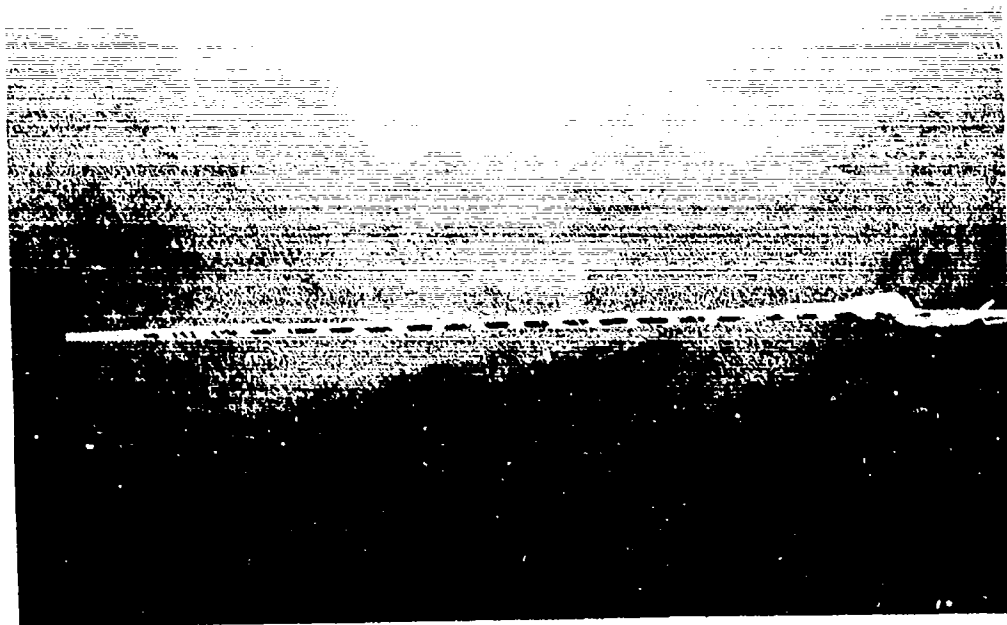
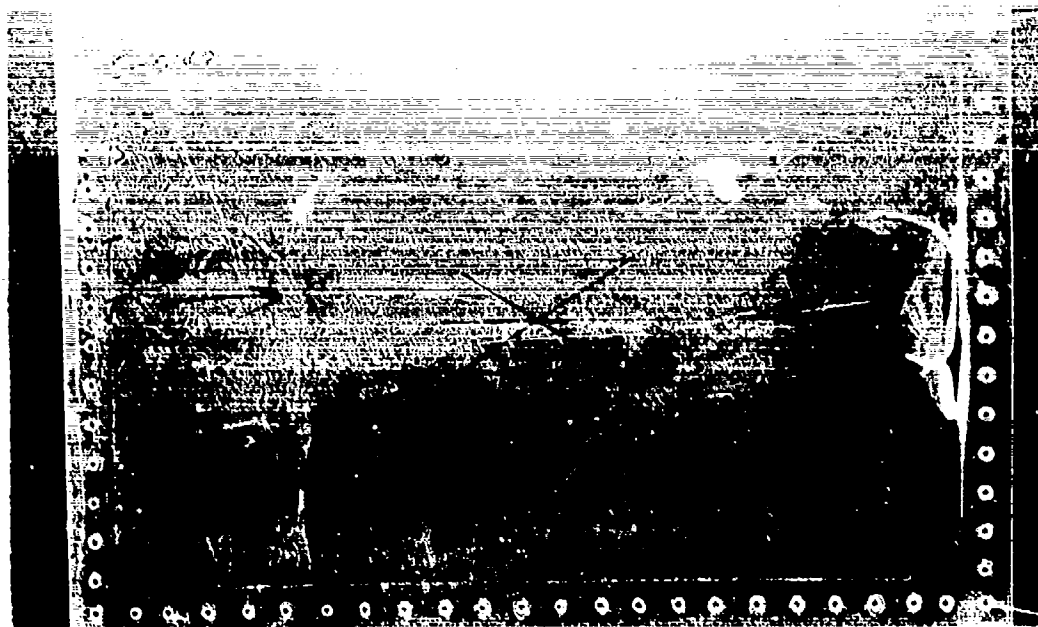


Figure A-9. Shot No. 5-0147; Panel impacted at the center edge; one-pound gelatin launched with a flat-on orientation at 202 m/s. a) front view; b) end view

a)



b)

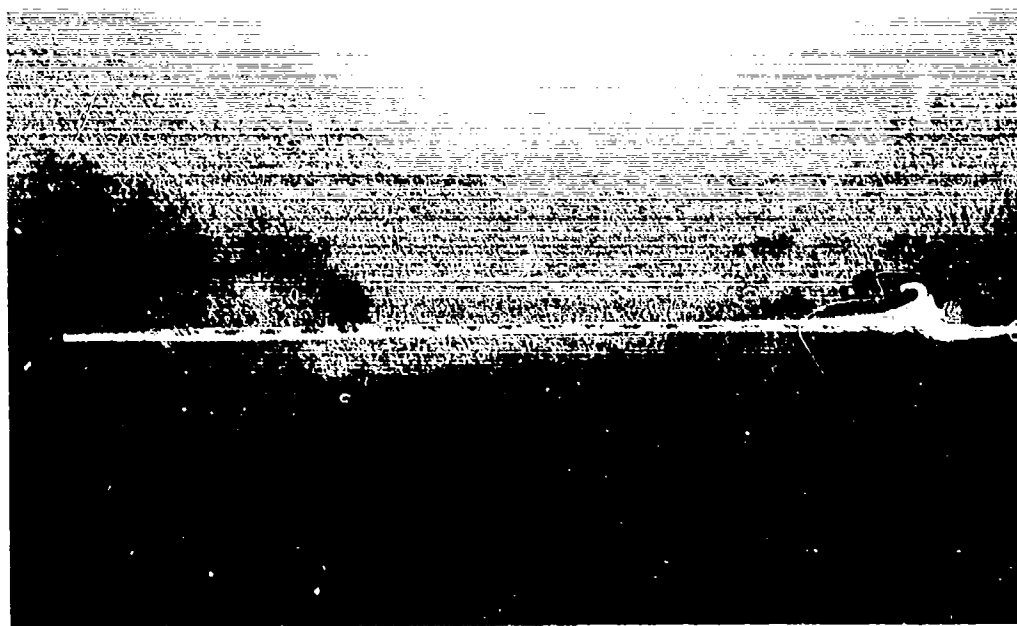
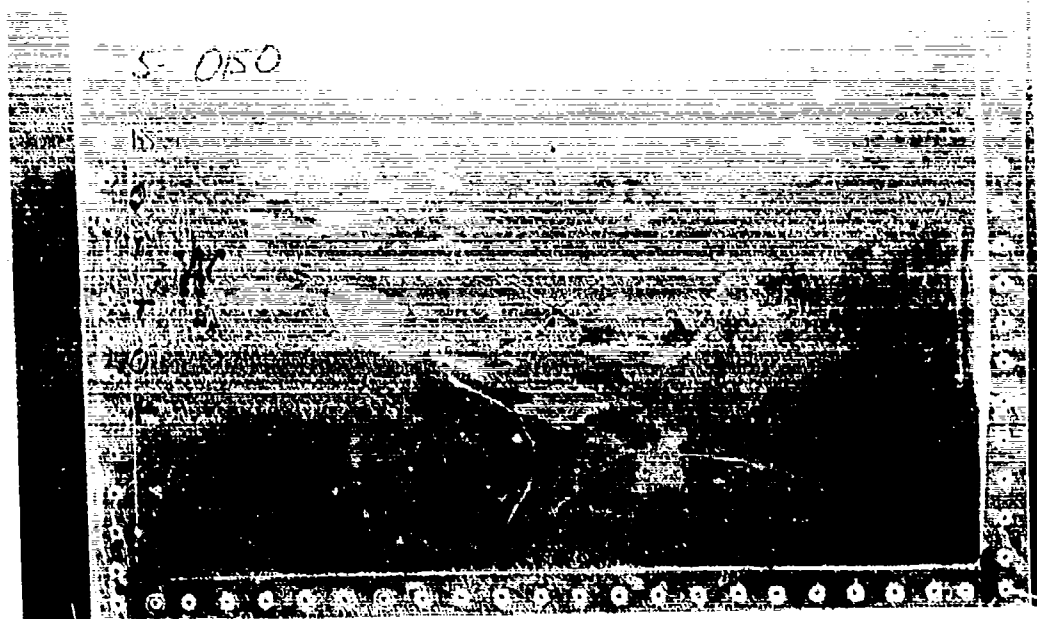


Figure A-10. Shot No. 5-0149; Panel impacted at the center edge; one-pound gelatin launched with a flat-on orientation at 206 m/s. a) front view; b) end view

a)



b)



Figure A-11. Shot No. 5-0150; Panel impacted at the center panel; one-pound gelatin launched with a flat-on orientation at 297 m/s. a) front view; b) end view

a)



b)

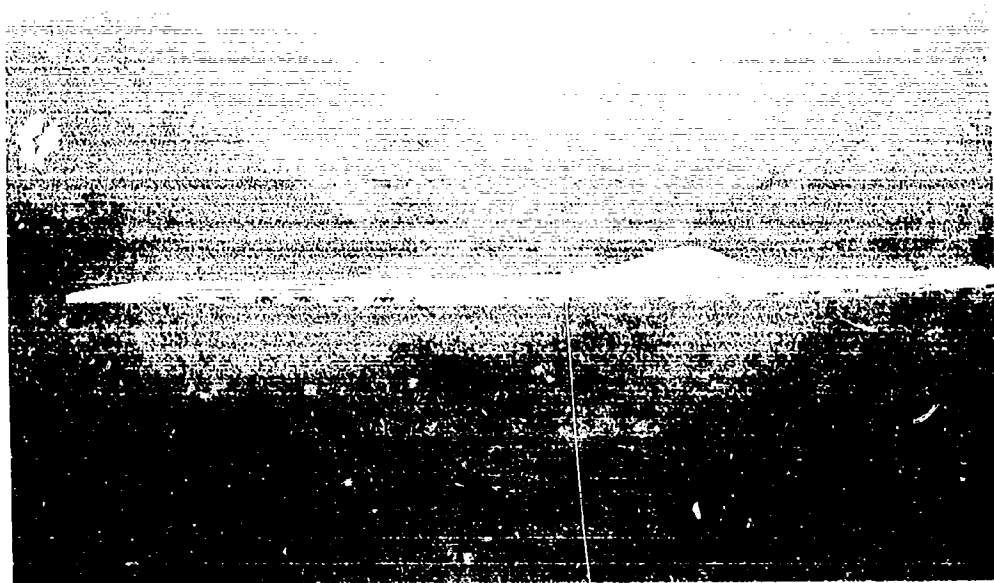
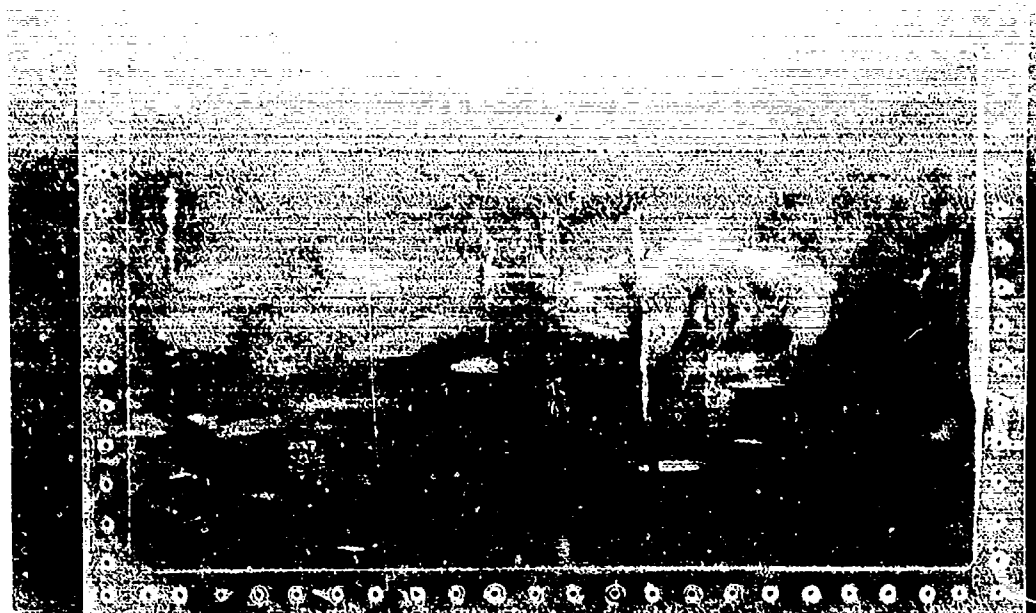


Figure A-12. Shot No. 5-0151; Panel impacted at the center panel; one-pound gelatin launched with a flat-on orientation at 307 m/s. a) front view; b) end view

a)

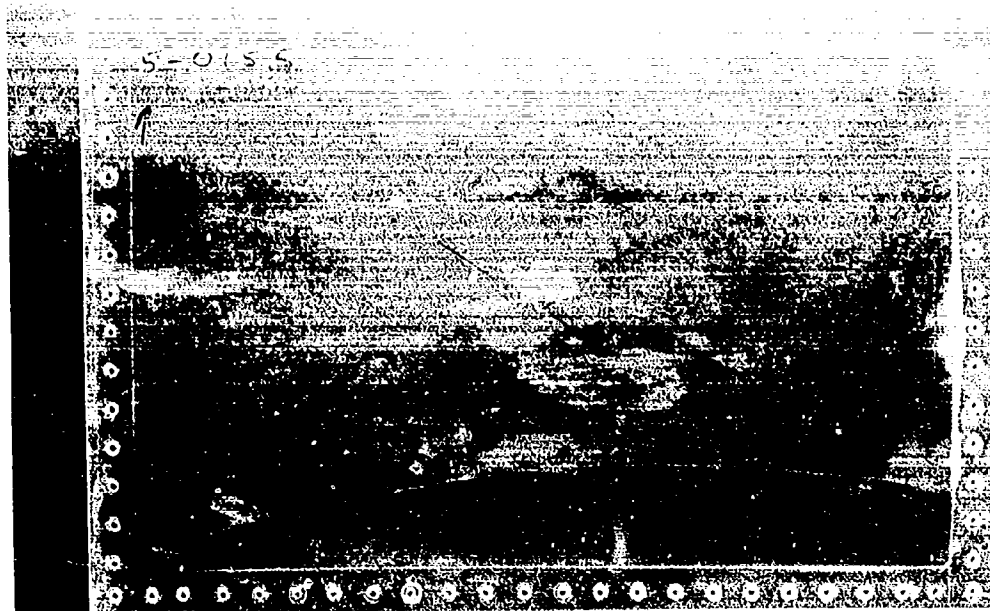


b)



Figure A-13. Shot No. 5-0152; Panel impacted at the center panel; one-pound gelatin launched with a flat-on orientation at 336 m/s. a) front view; b) end view

a)

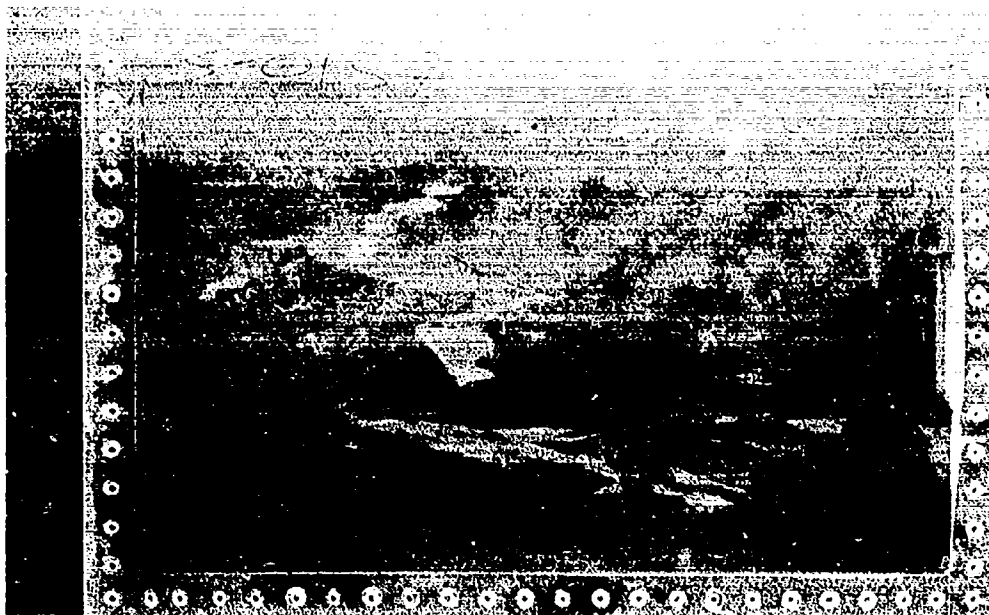


b)



Figure A-14. Shot No. 5-0155; Panel impacted at the center panel; one-pound gelatin launched with a side-on orientation at 292 m/s. a) front view; b) end view

a)



b)

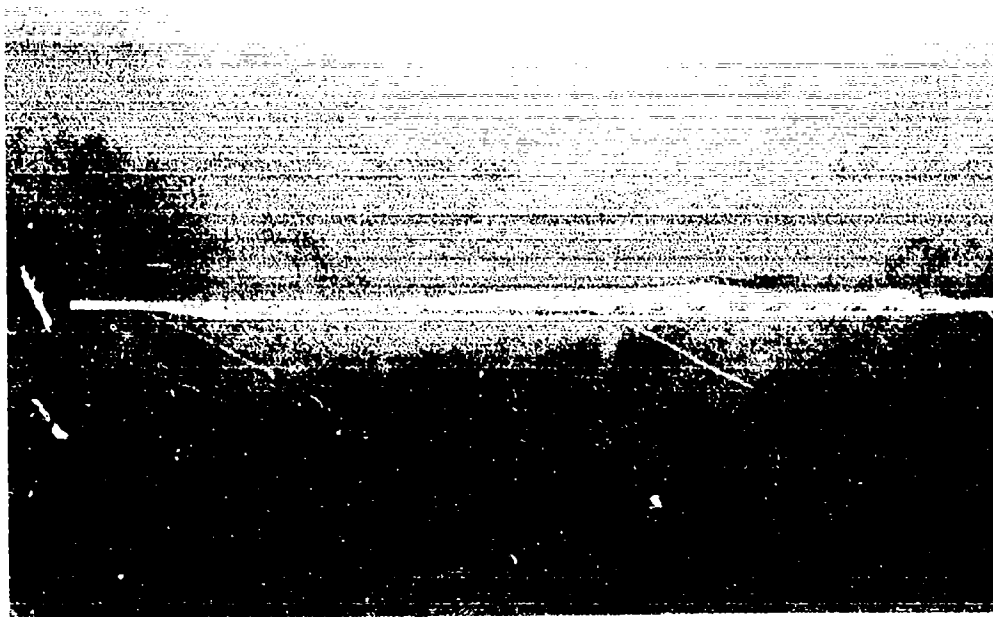
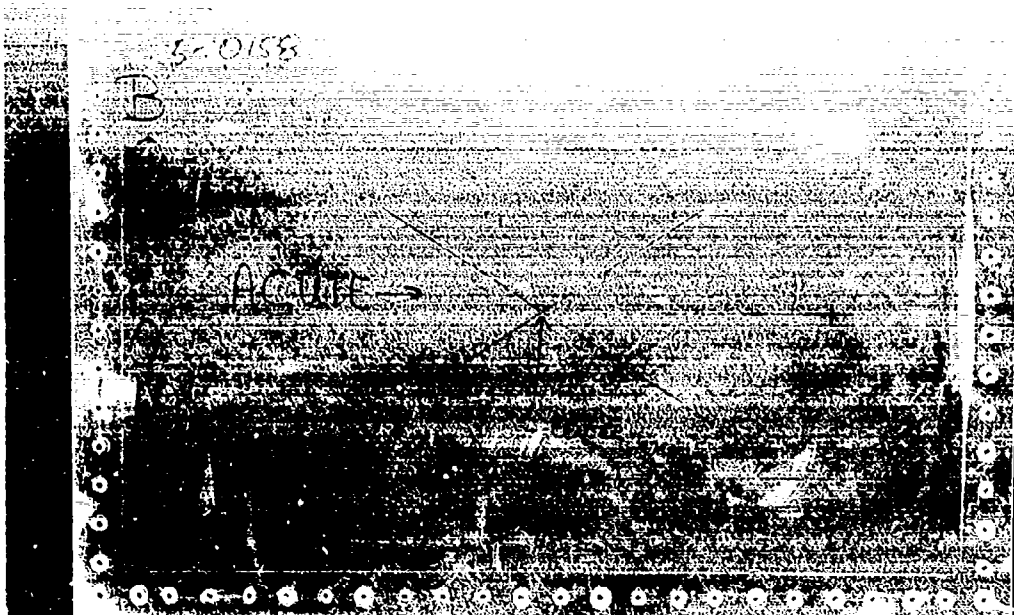


Figure A-15. Shot No. 5-0157; Panel impacted at the center panel; one-pound gelatin launched with a side-on orientation at 333 m/s. a) front view; b) end view



a)

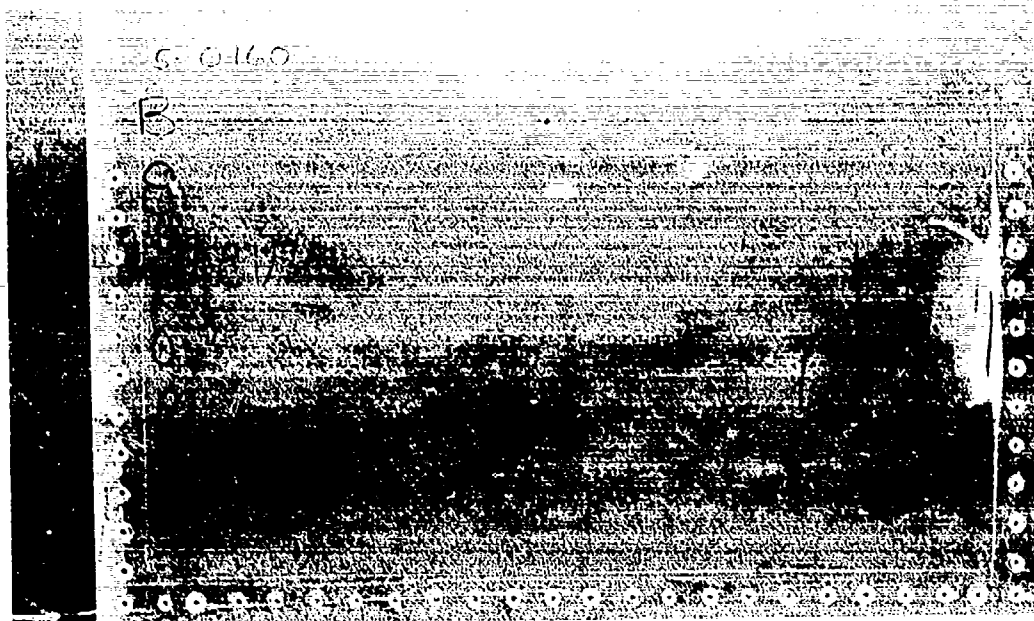


b)



Figure A-16. Shot No. 5-0158; Panel impacted at the center edge; one-pound gelatin launched with a side-on orientation at 210 m/s. a) front view; b) end view

a)



b)

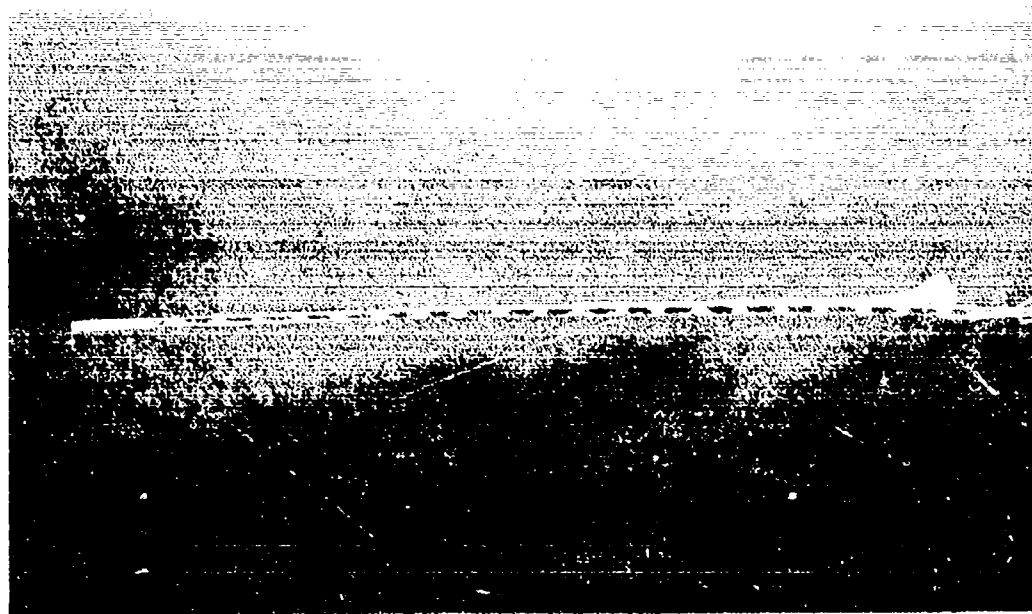
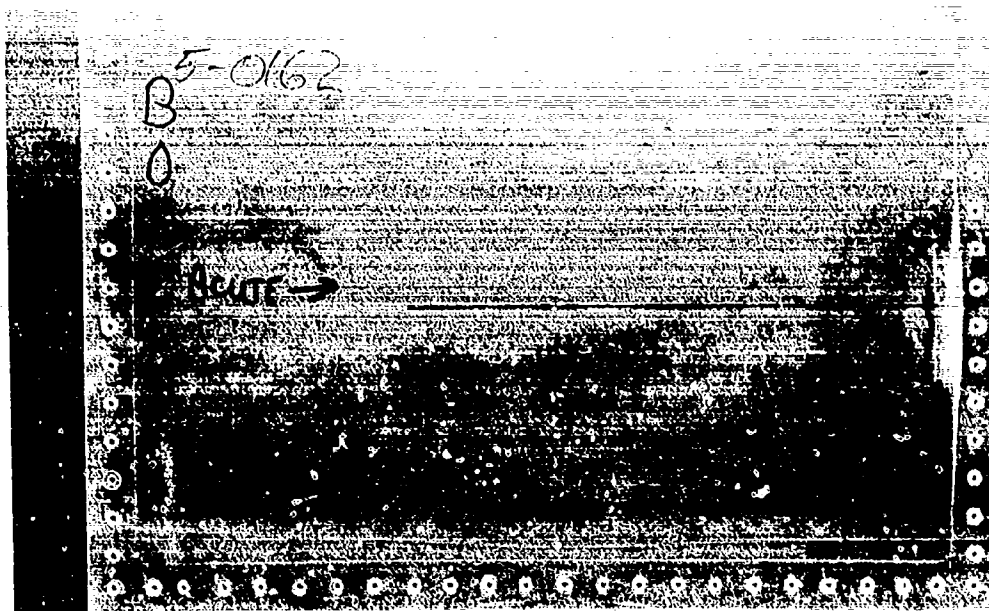


Figure A-17. Shot No. 5-0160; Panel impacted at the center edge; one-pound gelatin launched with a side-on orientation at 212 m/s. a) front view; b) end view

a)



b)

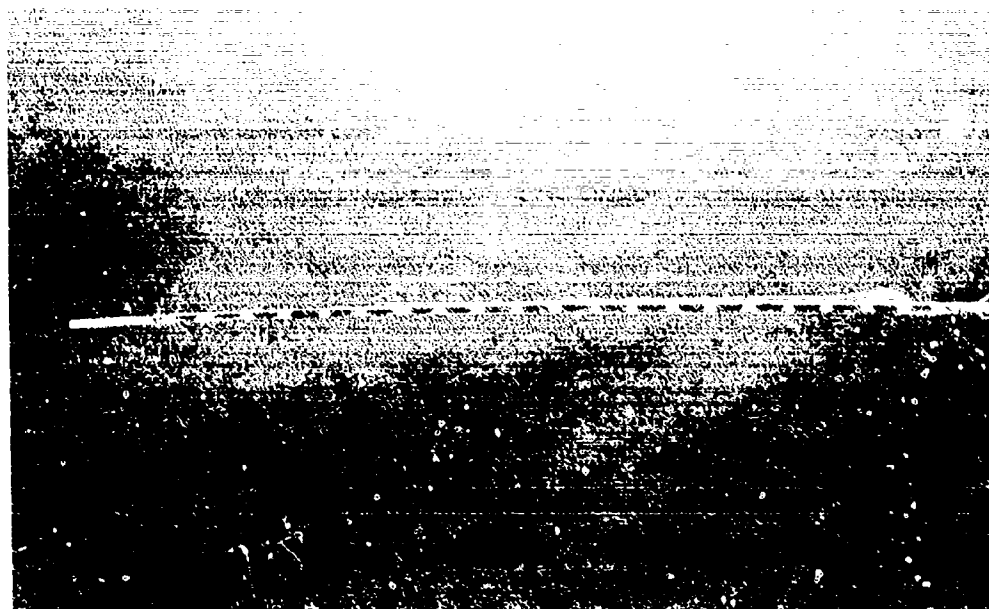
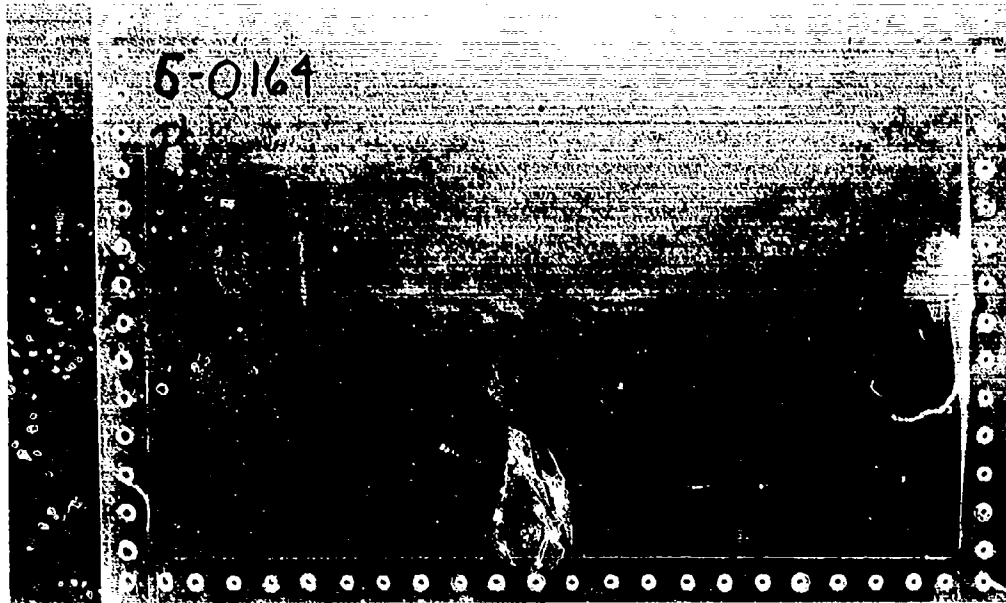


Figure A-18. Shot No. 5-0162; Panel impacted at the center edge; one-pound gelatin launched with a side-on orientation at 210 m/s. a) front view; b) end view

a)



b)

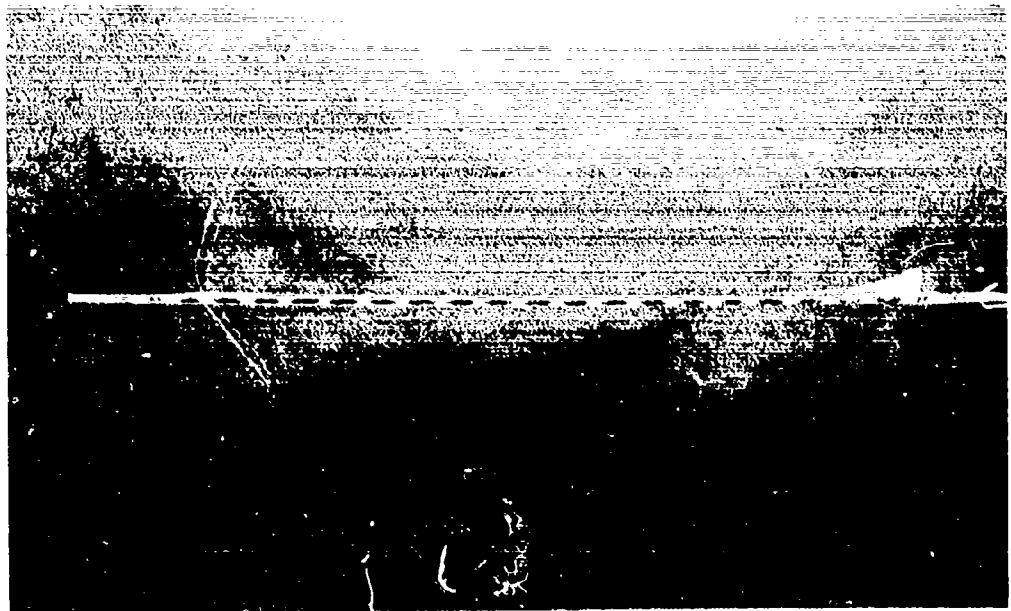
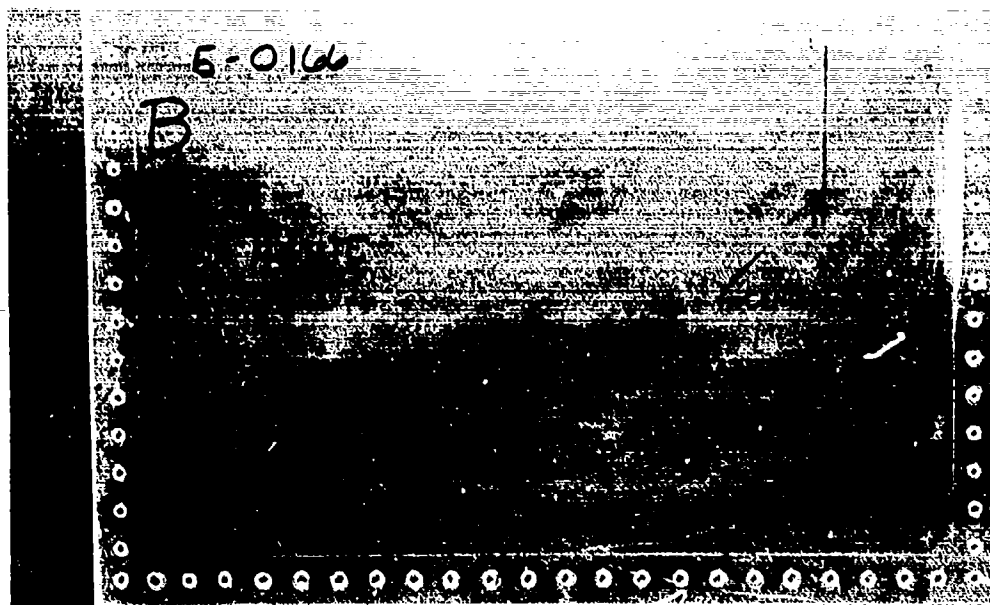


Figure A-19. Shot No. 5-0164; Panel impacted at the center edge; one-pound gelatin launched with a side-on orientation at 212 m/s. a) front view; b) end view

a)

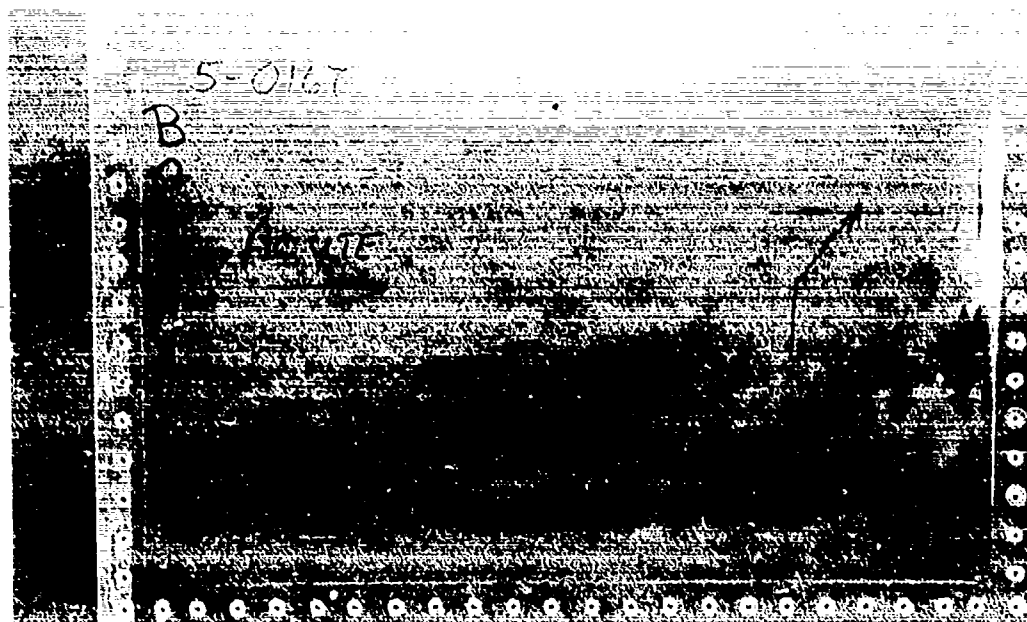


b)



Figure A-20. Shot No. 5-0166; Panel impacted at the down-stream corner; one-pound gelatin launched with a flat-on orientation at 181 m/s. a) front view; b) end view

a)



b)

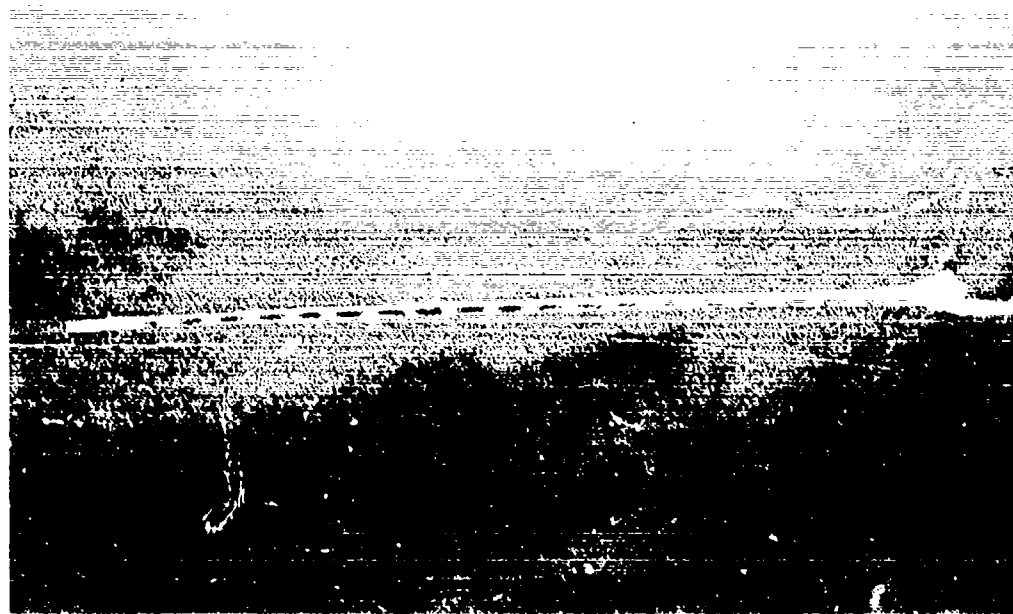


Figure A-21. Shot No. 5-0167; Panel impacted at the down-stream corner; one-pound gelatin launched with a flat-on orientation at 188 m/s. a) front view; b) end view

a)



b)



Figure A-22. Shot No. 5-0175; Panel impacted at the down-stream corner; one-pound gelatin launched with a side-on orientation at 237 m/s. a) front view; b) end view

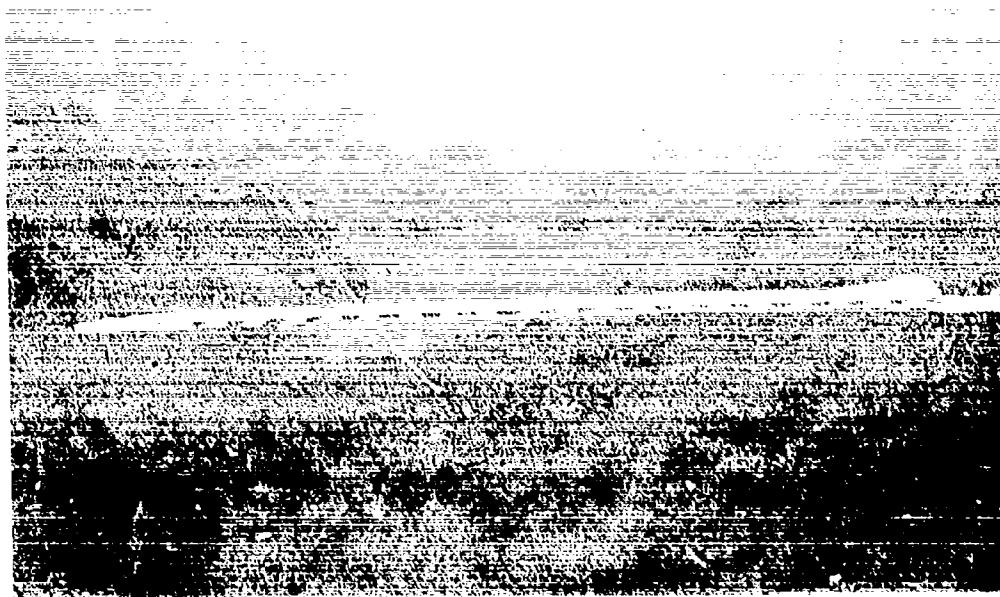
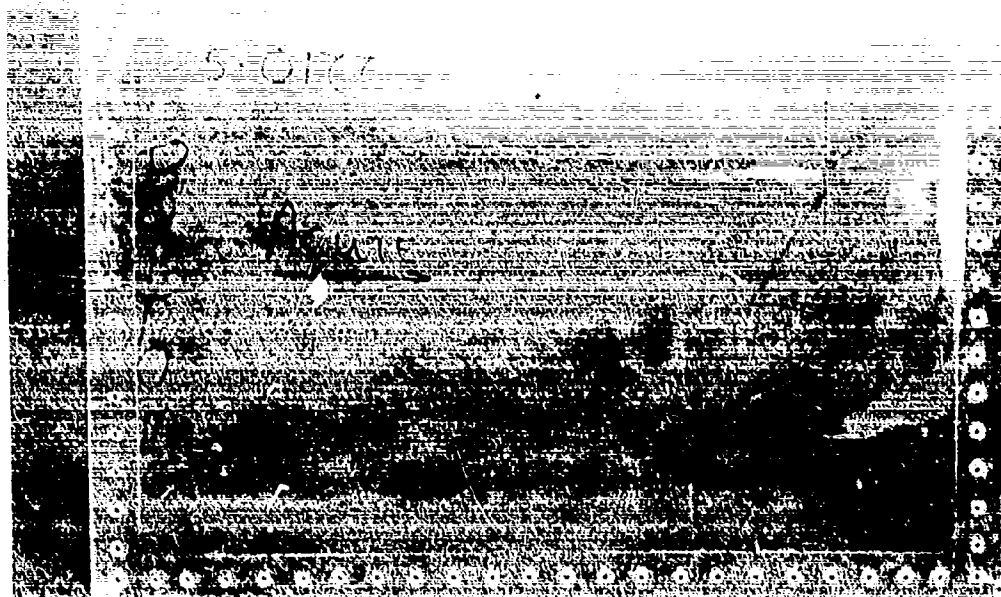


Figure A-23. Shot No. 5-0177; Panel impacted at the down-stream corner; one-pound gelatin launched with a side-on orientation at 232 m/s. a) front view; b) end view



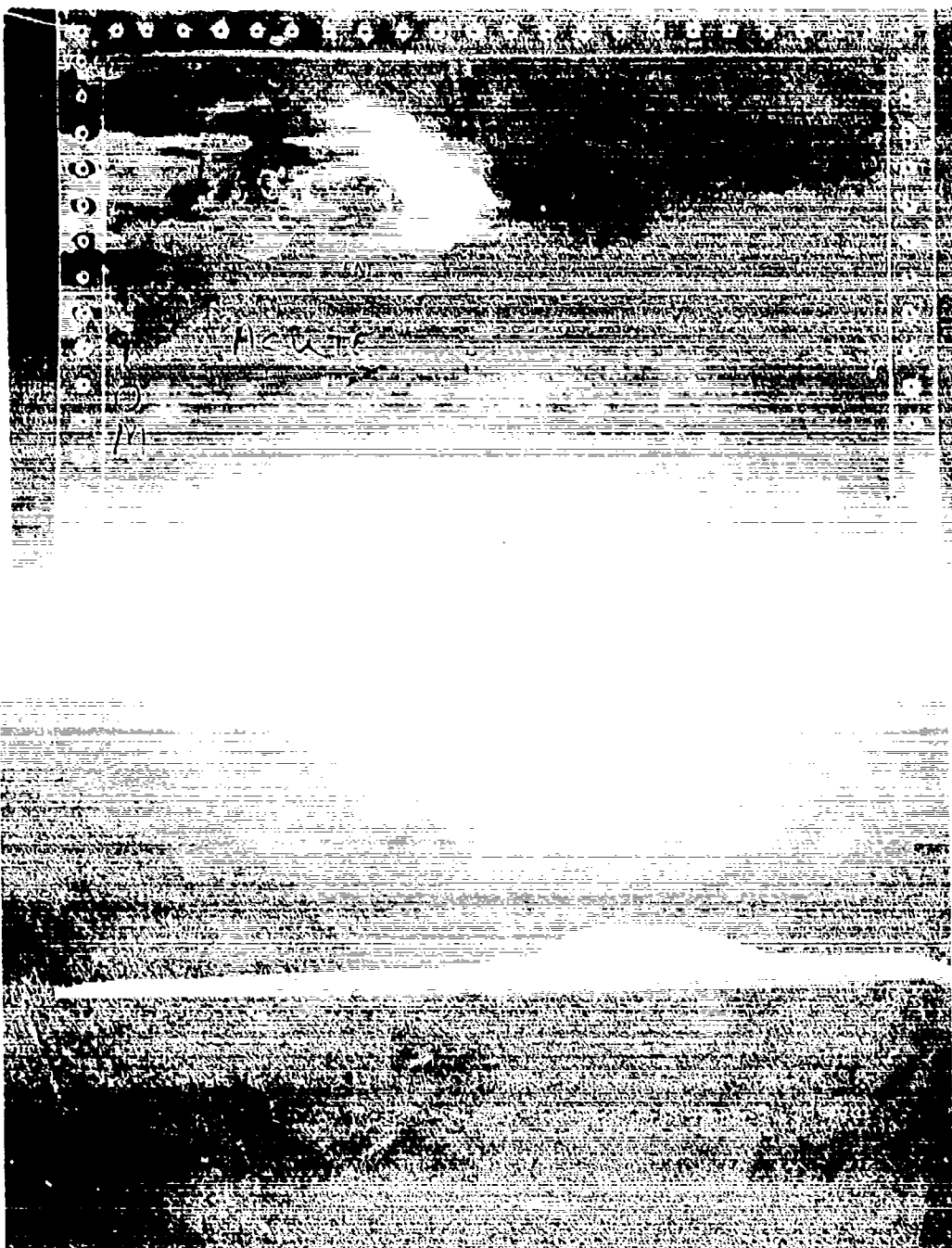
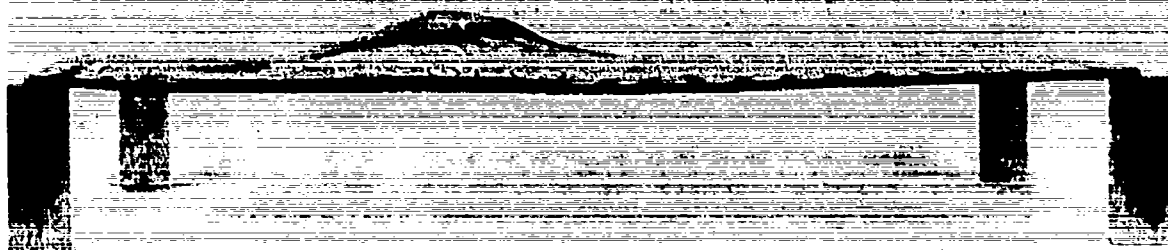


Figure A-24. Shot No. 5-0178; Panel impacted at the up-stream corner; one-pound gelatin launched with a flat-on orientation at 350 m/s. a) front view; b) end view

a)



b)



Figure A-25. Shot No. 5-0179; Panel impacted at the up-stream corner; one-pound gelatin launched with a flat-on orientation at 335 m/s. a) end view; b) end view

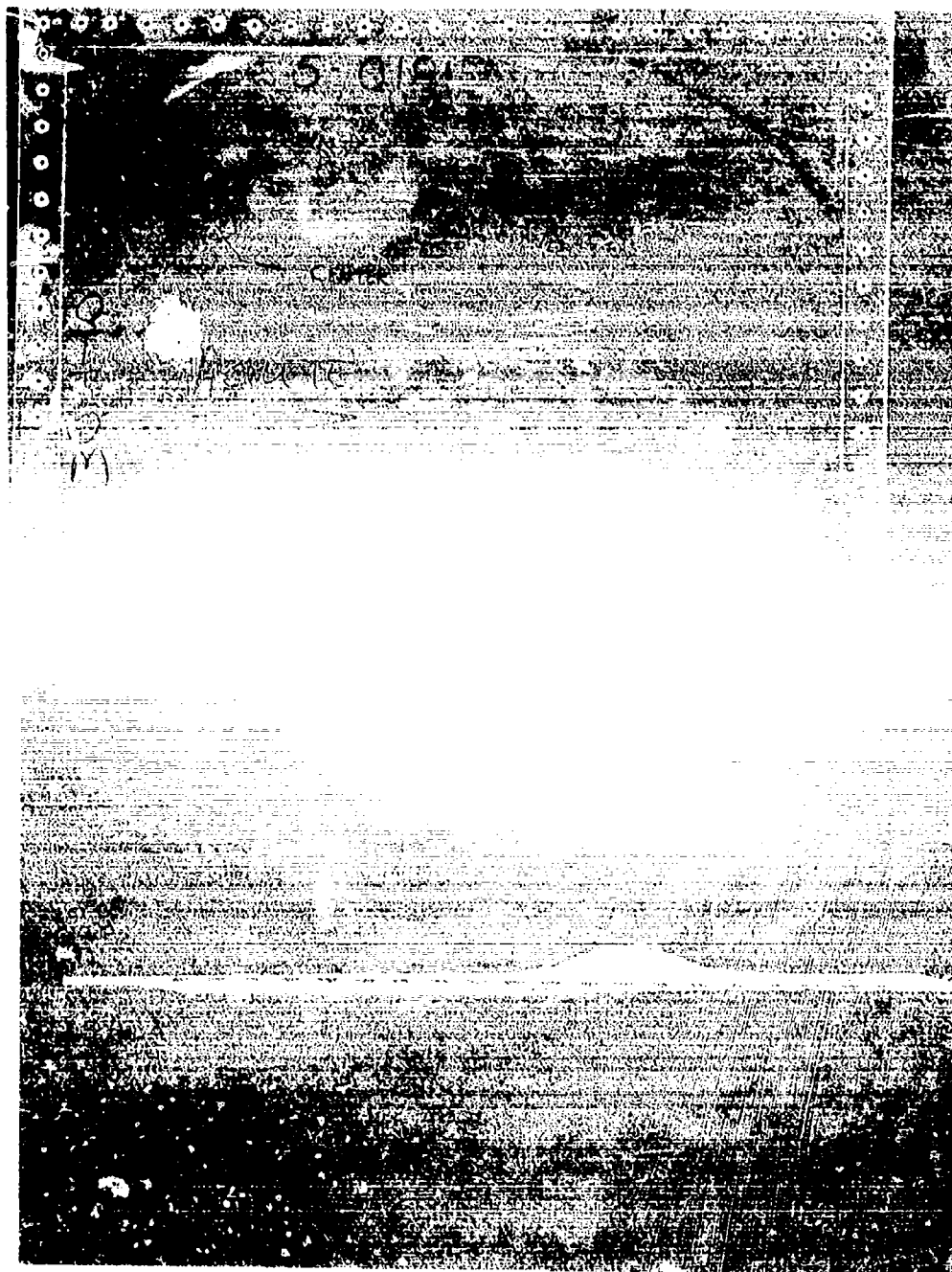


Figure A-26. Shot No. 5-0181; Panel impacted at the up-stream corner; one-pound gelatin launched with a flat-on orientation at 305 m/s. a) front view; b) end view



Figure A-27. Shot No. 5-0184; Panel impacted at the up-stream corner; one-pound gelatin launched with a side-on orientation at 306 m/s. a) front view; b) end view

## REFERENCES

1. Barber, J. P., and Wilbeck, J. S., "The Characterization of Bird Impacts on a Rigid Plate: Part I," AFFDL-TR-75-5 ADA021142, January 1975.
2. Barber, J. P., Taylor, H. R., and Wilbeck, J. S., "Bird Impact Forces and Pressures on Rigid and Compliant Targets," AFFDL-TR-77-60, ADA061-313, May 1978.
3. Challita, A., and Barber, J. P., "The Scaling of Bird Impact Loads," AFFDL-TR-79-3042, June 1979.
4. Wilbeck, T. S., "Impact Behavior of Low Strength Projectiles." AFML-TR-77-134, July 1978.
5. Peterson, R. L., and Barber, J. P., "Bird Impact Forces in Aircraft Windshield Design," AFFDL-TR-75-150, ADA026-628, March 1976.